

A High-Diversity Transceiver Design for MISO Broadcast Channels

Junyeong Seo, *Student Member, IEEE*, Youngchul Sung[†], *Senior Member, IEEE*,
and Hamid Jafarkhani, *Fellow, IEEE*

Abstract

In this paper, the outage behavior and diversity order of the mixture transceiver architecture for multiple-input single-output broadcast channels are analyzed. The mixture scheme groups users with closely-aligned channels and applies superposition coding and successive interference cancellation decoding to each group composed of users with closely-aligned channels, while applying zero-forcing beamforming across semi-orthogonal user groups. In order to enable such analysis, closed-form lower bounds on the achievable rates of a general multiple-input single-output broadcast channel with superposition coding and successive interference cancellation are newly derived. By employing channel-adaptive user grouping and proper power allocation, which ensures that the channel subspaces of user groups have angle larger than a certain threshold, it is shown that the mixture transceiver architecture achieves full diversity order in multiple-input single-output broadcast channels and opportunistically increases the multiplexing gain while achieving full diversity order. Furthermore, the achieved full diversity order is the same as that of the single-user maximum ratio transmit beamforming. Hence, the mixture scheme can provide reliable communication under channel fading for ultra-reliable low latency communication. Numerical results validate our analysis and show the outage superiority of the mixture scheme over conventional transceiver designs for multiple-input single-output broadcast channels.

Index Terms

Multiple-input single-output broadcast channels, outage probability, diversity order, successive interference cancellation, user grouping, mixture reception

[†]Corresponding author

J. Seo and Y. Sung are with Dept. of Electrical Engineering, KAIST, Daejeon 305-701, South Korea, and H. Jafarkhani is with Center for Pervasive Communications & Computing, UC Irvine, CA, USA. E-mail: jyseo@kaist.ac.kr, ysung@ee.kaist.ac.kr, and hamidj@uci.edu. This work was supported in part by Basic Science Research Program through the National Research Foundation of Korea (NRF) funded by the Ministry of Education (2013R1A1A2A10060852) and supported in part by the NSF Award CCF-1526780. This work is from a part of [1].

I. INTRODUCTION

The *multiple-input single-output (MISO) broadcast channel (BC) model* is an important channel model which captures modern cellular downlink communication in which a base station (BS) equipped with multiple transmit antennas simultaneously serves multiple receivers each equipped with a single receive antenna by using the spatial domain. Due to its importance it has been investigated extensively for more than a decade and major current wireless communication standards support MISO BC downlink communication [2]–[5]. It is known that the capacity region of a MISO BC can be achieved by dirty paper coding (DPC) [2]. However, because of the unavailability of practical dirty paper codes, simple linear downlink beamforming such as zero-forcing (ZF) beamforming is widely considered and used in practice [4], [6]. Although such simple linear beamforming is not a capacity-achieving scheme, it can yield good performance when it is combined with multi-user diversity and user scheduling [3], [4], [7]–[9]. That is, when the number of users in the cell is sufficiently large as compared to the number N of transmit antennas, the BS can select N users with nearly orthogonal channel vectors so that linear ZF downlink beamforming is sufficient. However, such orthogonality-based user scheduling for linear downlink beamforming may not be appropriate in certain cases. One example is the case in which the number of transmit antennas is large under rich scattering environments since it is difficult to simultaneously select multiple users with roughly orthogonal channels in this case [8]–[10]. Thus, for a MISO BC with a large number of transmit antennas it was proposed that the BS selects the users for simultaneous service arbitrarily and applies linear ZF beamforming [10]. Another emerging important example is *ultra-reliable low-latency communication (URLLC)* for fast machine-type communication in 5G. In the case of URLLC, such orthogonality-based user scheduling induces extra delay in communication since the users requiring immediate data transmission may not have channel vectors nearly orthogonal to each other or to other on-going overlapping data users under spatial multiplexing. Hence, it is preferred that the BS immediately schedules the users requiring low-latency data transmission regardless of their channel vectors' mutual orthogonality. In both examples, the channel vectors of the scheduled users are not guaranteed to be nearly orthogonal and the performance of linear ZF beamforming can be severely degraded since the channel vectors of some of the scheduled users can be closely aligned and the channel alignment causes poor conditioning of the channel matrix for ZF inversion.

Recently, inspired by the usefulness of superposition coding and successive interference cancellation (SIC) decoding in non-orthogonal multiple access (NOMA) [11], [12], a mixture (or hybrid) transceiver architecture was considered for MISO BCs to overcome the drawback of the fully linear ZF downlink

beamforming based on *user grouping* and *mixture of linear and non-linear reception* [13], [14]. The basic idea of the mixture transceiver architecture is as follows. Under the assumption of independent and identically distributed (i.i.d.) realization of K channel vectors in K -user MISO downlink, if the channel vectors of some users are closely aligned, the performance of ZF beamforming is severely degraded. However, if we group the closely-aligned users and apply superposition coding and non-linear SIC decoding for each closely-aligned user group while applying ZF beamforming across roughly-orthogonal user-groups, the performance degradation by the full ZF beamforming can be alleviated. Preliminary study on such user grouping and mixture transreception was performed on the two-user grouping case, where intra-group rate analysis is rather simple [13], [14]. In [13], Pareto-optimal beam design is considered for the two-user grouping case, the beam vectors and corresponding rates are numerically obtained, and the performance of the mixture scheme is compared with the full ZF beamforming numerically. In [14], under the assumption of two users in each group, closed-form beam vectors are obtained to minimize the transmit power under a signal-to-interference-plus-noise ratio (SINR) constraint for each user based on quasi-degradation, and it was shown that such a mixture architecture based on two-user grouping increases the diversity order by one as compared to the conventional ZF downlink beamforming. Although such two-user grouping for the mixture transceiver architecture is tractable, it has limitation in diversity order improvement. (The related idea of hierarchical coding and user grouping was discussed in the dual scenario of multiple access channel in [15], and the idea of user grouping and inter-group zero forcing was also considered in [16] using the intra-group processing of a classical spatial multiplexing from a capacity perspective.)

In this paper, we fully generalize the mixture transceiver architecture for general MISO BCs. The contributions of the paper are summarized as follows:

- In order to enable analysis of the outage probability and diversity order of the mixture transceiver architecture, we derive a new lower bound on the achievable rate of each user in closed form in terms of each user's channel norm for a MISO BC with superposition coding and SIC decoding with an arbitrary number of users.
- We propose a channel-adaptive user grouping method which ensures a condition for the channel subspace angle property for the constructed user groups and a power allocation method necessary for achievability of full diversity order.
- Combining the newly derived achievable rate result and the property of the proposed adaptive user grouping method, we derive the diversity order of the mixture transceiver architecture, and show that *the mixture transceiver architecture achieves full diversity order in MISO BCs, which is the same as*

that of the single-user maximal ratio transmit (MRT) beamforming, and furthermore it opportunistically increases multiplexing gain.

- We further investigate the related issues such as diversity-and-multiplexing trade-off associated with the mixture scheme, impact of imperfect channel state information (CSI), etc.

Notations: Vectors and matrices are written in boldface with matrices in capitals. All vectors are column vectors. For a matrix \mathbf{A} , \mathbf{A}^* , \mathbf{A}^H , \mathbf{A}^T and $\text{Tr}(\mathbf{A})$ indicate the complex conjugate, conjugate transpose, transpose and trace of \mathbf{A} , respectively, and $\mathcal{C}(\mathbf{A})$ and $\mathcal{C}^\perp(\mathbf{A})$ denotes the linear subspace spanned by the columns of \mathbf{A} and its orthogonal complement, respectively. $\mathbf{\Pi}_{\mathbf{A}}$ and $\mathbf{\Pi}_{\mathbf{A}}^\perp$ are the projection matrices to $\mathcal{C}(\mathbf{A})$ and $\mathcal{C}^\perp(\mathbf{A})$, respectively. $[\mathbf{a}_1, \dots, \mathbf{a}_n]$ denotes the matrix composed of column vectors $\mathbf{a}_1, \dots, \mathbf{a}_n$. $\|\mathbf{a}\|$ represents the 2-norm of vector \mathbf{a} . \mathbf{I}_n denotes the identity matrix of size n (the subscript is omitted when unnecessary). $\mathbf{x} \sim \mathcal{CN}(\boldsymbol{\mu}, \boldsymbol{\Sigma})$ means that random vector \mathbf{x} is circularly-symmetric complex Gaussian distributed with mean vector $\boldsymbol{\mu}$ and covariance matrix $\boldsymbol{\Sigma}$.

II. THE CHANNEL MODEL AND PRELIMINARIES

A. The Channel Model

In this paper, we consider a Gaussian MISO BC composed of a transmitter with N transmit antennas and K single-antenna users (i.e., receivers), where the number of users is less than or equal to the number of transmit antennas, i.e., $K \leq N$. The received signal y_k at the k -th user is given by

$$y_k = \mathbf{h}_k^H \mathbf{x} + n_k, \quad k = 1, 2, \dots, K, \quad (1)$$

where \mathbf{x} is the $N \times 1$ transmit signal vector at the transmitter with the total transmit power $P_t = \mathbb{E}\{\mathbf{x}\mathbf{x}^H\}$, n_k is the additive white Gaussian noise (AWGN) at the k -th user, i.e., $n_k \sim \mathcal{CN}(0, \sigma^2)$ with σ^2 set to 1 for simplicity, and \mathbf{h}_k is the $N \times 1$ (conjugated) channel vector from the transmitter to the k -th user following independent Rayleigh fading, i.e.,

$$\mathbf{h}_k = [h_{k1}, h_{k2}, \dots, h_{kN}]^T \stackrel{i.i.d.}{\sim} \mathcal{CN}(\mathbf{0}, 2\mathbf{I}). \quad (2)$$

Here, we set $2\mathbf{I}$ as the covariance matrix for convenience so that both real and imaginary components of each element of \mathbf{h}_k have variance one and thus $\|\mathbf{h}_k\|^2$ has the chi-square distribution of degrees of freedom $2N$. Different scaling can be absorbed into the transmit power. Concatenating all the received signals y_1, \dots, y_K , we can write the matrix model for the received signals as

$$\mathbf{y} = \mathbf{H}^H \mathbf{x} + \mathbf{n}, \quad (3)$$

where $\mathbf{y} = [y_1, y_2, \dots, y_K]^T$, $\mathbf{n} = [n_1, n_2, \dots, n_K]^T$, and $\mathbf{H} = [\mathbf{h}_1, \mathbf{h}_2, \dots, \mathbf{h}_K]$. We assume that the channel state information (CSI) \mathbf{H} is available at the transmitter. Due to the assumption of $K \leq N$, the $K \times N$ overall channel matrix \mathbf{H}^H is a fat matrix and hence it is right-invertible so that conventional ZF transmit beamforming is feasible. Design of the signal vector \mathbf{x} and receiver processing based on $\{y_1, y_2, \dots, y_K\}$ will be explained in the subsequent sections.

B. Preliminaries: Reliability and Diversity Order

Channel fading is inherent in wireless communication, and communication reliability under channel fading is dependent on the diversity order of the communication channel. Consider the well-known single-user MRT beamforming with multiple transmit antennas. The corresponding channel model is given by the channel model (1) with only a single user, i.e., $K = 1$. For MRT beamforming, we have $\mathbf{x} = \frac{\mathbf{h}_1}{\|\mathbf{h}_1\|} \sqrt{p_1} s_1$ with $\mathbb{E}\{|s_1|^2\} = 1$. The resulting equivalent single-input single-output (SISO) channel and rate are respectively given by

$$y_1 = \|\mathbf{h}_1\| \sqrt{p_1} s_1 + n_1 \quad \text{and} \quad R_1 = \log(1 + \|\mathbf{h}_1\|^2 \text{SNR}), \quad \text{SNR} := \frac{p_1}{\sigma^2}, \quad (4)$$

where the probability density function (pdf) of $\|\mathbf{h}_1\|^2 = |h_{11}|^2 + \dots + |h_{1N}|^2$ is given by the chi-square distribution with degree of freedom $2N$ since it is the sum of the squares of $2N$ standard normal random variables:

$$f_{\|\mathbf{h}_1\|^2}(x) = \frac{1}{2^N (N-1)!} x^{N-1} e^{-x/2} = \frac{1}{2^N (N-1)!} x^{N-1} + o(x^{N-1}), \quad \text{as } x \rightarrow 0, \quad (5)$$

where $o(\cdot)$ is the small o notation. Communication outage is defined as the event that the channel cannot support a given target rate R^{th} , and the corresponding outage probability is given by $P_{out} = \Pr\{R_1 < R^{th}\}$ [17]. Then, the diversity of order of the channel is defined as [17]

$$D := - \lim_{\text{SNR} \rightarrow \infty} \frac{\log P_{out}}{\log \text{SNR}}. \quad (6)$$

In the single-user MRT beamforming case, the outage probability is given by $P_{out} = \Pr\left\{\|\mathbf{h}_1\|^2 \leq \frac{2^{R^{th}} - 1}{\text{SNR}}\right\} \approx \frac{(2^{R^{th}} - 1)^N}{2^N N! \text{SNR}^N}$ [17], and hence the diversity order in this case is N . That is, the outage probability decays as SNR^{-N} , as SNR increases. Note that in the case of a Rayleigh-fading SISO channel with a single transmit antenna $N = 1$, the pdf (5) reduces to $f_{|h_{11}|^2}(x) = \frac{1}{2} e^{-x/2}$, and the diversity order reduces to one. Hence, MRT beamforming with N transmit antennas increases the diversity order by N times as compared to the SISO case.

Now, consider the general Gaussian MISO BC (1) with ZF downlink beamforming for $K = N$. In the ZF beamforming case, the overall transmit signal \mathbf{x} is given by $\mathbf{x} = \mathbf{w}_1^{ZF} \sqrt{p_1} s_1 + \cdots + \mathbf{w}_K^{ZF} \sqrt{p_K} s_K$, where \mathbf{w}_k^{ZF} and s_k are the ZF beam vector and data symbol for the k -th user with $\|\mathbf{w}_k^{ZF}\|^2 = 1$ and $\mathbb{E}\{|s_k|^2\} = 1$, respectively. Here, the ZF beam vector \mathbf{w}_k^{ZF} lies in $\mathcal{C}^\perp([\mathbf{h}_1, \cdots, \mathbf{h}_{k-1}, \mathbf{h}_{k+1}, \cdots, \mathbf{h}_K])$ so that $\mathbf{h}_i^H \mathbf{w}_k^{ZF} = 0$ for all $i \neq k$. Then, the resulting SISO channel for the k -th user is given by

$$y_k = \mathbf{h}_k^H \mathbf{w}_k^{ZF} \sqrt{p_k} s_k + n_k. \quad (7)$$

In the case of independent Rayleigh fading, the channel vector \mathbf{h}_k and the remaining $\{\mathbf{h}_1, \cdots, \mathbf{h}_{k-1}, \mathbf{h}_{k+1}, \cdots, \mathbf{h}_K\}$ are independent. Hence, the one-dimensional subspace $\mathcal{C}^\perp([\mathbf{h}_1, \cdots, \mathbf{h}_{k-1}, \mathbf{h}_{k+1}, \cdots, \mathbf{h}_K])$ is also independent of \mathbf{h}_k , and hence \mathbf{h}_k is circularly-symmetric Gaussian distributed over \mathbb{C}^N with respect to a reference direction of $\mathcal{C}^\perp([\mathbf{h}_1, \cdots, \mathbf{h}_{k-1}, \mathbf{h}_{k+1}, \cdots, \mathbf{h}_K])$. Therefore, taking the inner product between \mathbf{h}_k and the unit-norm vector $\mathbf{w}_k^{ZF} \in \mathcal{C}^\perp([\mathbf{h}_1, \cdots, \mathbf{h}_{k-1}, \mathbf{h}_{k+1}, \cdots, \mathbf{h}_K])$ is equivalent to taking only one component out of N complex Gaussian components, and thus $|\mathbf{h}_k^H \mathbf{w}_k^{ZF}|^2$ has the same pdf as $f_{|h_{11}|^2}(x) = \frac{1}{2}e^{-x/2}$. Hence, the corresponding diversity order for the k -th user is simply one for all k [14] as in the SISO Rayleigh fading channel. Thus, ZF downlink beamforming for MISO BCs loses the diversity gain possibly obtainable from multiple transmit antennas.

Note that if \mathbf{h}_k is perfectly orthogonal to $\mathbf{h}_1, \cdots, \mathbf{h}_{k-1}, \mathbf{h}_{k+1}, \cdots, \mathbf{h}_K$, then $\mathcal{C}^\perp([\mathbf{h}_1, \cdots, \mathbf{h}_{k-1}, \mathbf{h}_{k+1}, \cdots, \mathbf{h}_K])$ is perfectly aligned with \mathbf{h}_k and hence in this case we have $\mathbf{h}_k^H \mathbf{w}_k^{ZF} = \|\mathbf{h}_k\|$. In this case, the resulting SISO channel for the k -th user is the same as that of the MRT beamforming single-user channel in (4). Furthermore, suppose that the angle between \mathbf{h}_k and one-dimensional subspace $\mathcal{C}^\perp([\mathbf{h}_1, \cdots, \mathbf{h}_{k-1}, \mathbf{h}_{k+1}, \cdots, \mathbf{h}_K])$ is equal to or less than a certain fixed threshold α . Then, we have $|\mathbf{h}_k^H \mathbf{w}_k^{ZF}| \geq \|\mathbf{h}_k\| \cos \alpha$. Since $\cos \alpha$ is a constant, the pdf of $|\mathbf{h}_k^H \mathbf{w}_k^{ZF}|^2$ is a certain scaled version of that of $\|\mathbf{h}_k\|^2$ (the meaning of this statement will become clear in later sections), and the outage behavior for the k -th user in this case should be the same as that of the MRT single-user case as SNR increases without bound. Reflecting this, one can recognize that the degradation of diversity order of ZF beamforming for a MISO BC with independent channel fading results from the uncontrolled and arbitrary angle between \mathbf{h}_k and $\mathcal{C}^\perp([\mathbf{h}_1, \cdots, \mathbf{h}_{k-1}, \mathbf{h}_{k+1}, \cdots, \mathbf{h}_K])$.

III. THE MIXTURE TRANSCEIVER ARCHITECTURE

In this section, motivated by the discussion in the previous section, we consider the mixture transceiver architecture for Gaussian MISO BCs [13], [14] in order to overcome the diversity drawback of ZF downlink beamforming. The mixture architecture is based on user grouping and mixture of linear ZF and

non-linear SIC reception. First, user grouping is performed to group users with closely-aligned channel vectors. Then, superposition coding and SIC are applied to the users with closely-aligned channel vectors in each group, whereas ZF beamforming is applied across groups. In order to fully enhance the diversity order of the resulting individual user channel, we generalize the mixture architecture by adopting adaptive user grouping, which yields channel-dependent groups and enforces the angle between the subspace of each group and the orthogonal complement of the union of all other groups' subspaces to be less than a certain threshold so that inter-group ZF beamforming does not harm the overall diversity order.

From here on, we explain the mixture transceiver architecture with the proposed user grouping method in detail. We consider the MISO BC explained in Section II-A as our channel model. We assume the following for our transceiver architecture:

A.1 (User Grouping): First, we group the K users into N_g groups. The constructed groups are denoted by the sets $\mathcal{G}_1, \mathcal{G}_2, \dots, \mathcal{G}_{N_g}$ such that $\mathcal{G}_i \cap \mathcal{G}_j = \emptyset$ for $i \neq j$ and $\bigcup_{j=1}^{N_g} \mathcal{G}_j = \{1, 2, \dots, K\}$. User grouping is adaptive in the sense that the number of groups can vary and the number of members in each group can vary from one to K , depending on the channels such that $\sum_{j=1}^{N_g} |\mathcal{G}_j| = K$. The constructed groups satisfy a certain subspace angle property in order to apply inter-group ZF beamforming without degrading the diversity order. The detailed method for user grouping will be presented in Section III-B.

A.2 (Inter-Group Beamforming): With the constructed groups, in order to control inter-group interference, we apply ZF beamforming across the constructed groups. With this inter-group ZF beamforming, the inter-group interference across the groups is zero.

A.3 (Intra-Group Processing: Superposition Coding and SIC): With the constructed groups, for intra-group processing we apply superposition coding and SIC decoding to each and every group with more than one user.

Under the aforementioned transceiver architecture, the transmit signal \mathbf{x} of the transmitter can be expressed as

$$\mathbf{x} = \sum_{j=1}^{N_g} \mathbf{\Pi}^{(j)} \sum_{i \in \mathcal{G}_j} \sqrt{p_i^{(j)}} \mathbf{w}_i^{(j)} s_i^{(j)}, \quad (8)$$

where $s_i^{(j)}$ is the transmit symbol from $\mathcal{CN}(0, 1)$ for User i in group \mathcal{G}_j , $\mathbf{w}_i^{(j)}$ is the $N \times 1$ intra-group beamforming vector for User i in group \mathcal{G}_j out of the feasible set $\widetilde{\mathcal{W}} := \{\mathbf{w} \mid \|\mathbf{\Pi}^{(j)} \mathbf{w}\|^2 \leq 1\}$, $p_i^{(j)}$ is the power assigned to User i in group \mathcal{G}_j , and $\mathbf{\Pi}^{(j)}$ is the inter-group ZF projection matrix for group \mathcal{G}_j . We assume that the total transmit power P_t is divided such that $|\mathcal{G}_j| \times P_t/K$ is allocated to group \mathcal{G}_j .

Then, from (1) the received signal at User i in group \mathcal{G}_j can be written as

$$y_i^{(j)} = \mathbf{h}_i^{(j)H} \left(\mathbf{\Pi}^{(j)} \sum_{i \in \mathcal{G}_j} \sqrt{p_i^{(j)}} \mathbf{w}_i^{(j)} s_i^{(j)} \right) + n_i^{(j)} \stackrel{(a)}{=} \left(\mathbf{\Pi}^{(j)} \mathbf{h}_i^{(j)} \right)^H \left(\sum_{i \in \mathcal{G}_j} \sqrt{p_i^{(j)}} \mathbf{w}_i^{(j)} s_i^{(j)} \right) + n_i^{(j)}, \quad (9)$$

where $\mathbf{h}_i^{(j)}$ is the $N \times 1$ channel vector between the transmitter and User i in group \mathcal{G}_j , and $n_i^{(j)} \sim \mathcal{CN}(0, 1)$ is the AWGN at User i in group \mathcal{G}_j (here, the single user index k in (1) is properly mapped to the two indices: intra-group user index i and group index j). The inter-group ZF projection matrix $\mathbf{\Pi}^{(j)}$ is given by $\mathbf{\Pi}^{(j)} = \mathbf{\Pi}_{\tilde{\mathbf{H}}_j}^\perp$, where $\tilde{\mathbf{H}}_j$ is the matrix composed of all channel vectors except the channel vectors of the users in group \mathcal{G}_j , i.e.,

$$\tilde{\mathbf{H}}_j := [\mathbf{h}_1^{(1)} \dots \mathbf{h}_{|\mathcal{G}_1|}^{(1)}, \dots, \mathbf{h}_1^{(j-1)} \dots \mathbf{h}_{|\mathcal{G}_{j-1}|}^{(j-1)}, \mathbf{h}_1^{(j+1)} \dots \mathbf{h}_{|\mathcal{G}_{j+1}|}^{(j+1)}, \dots, \mathbf{h}_1^{(N_g)} \dots \mathbf{h}_{|\mathcal{G}_{N_g}|}^{(N_g)}]. \quad (10)$$

Due to the inter-group ZF beamforming, there is no inter-group interference in (9), and the property of an orthogonal projection matrix, $(\mathbf{\Pi}_{\tilde{\mathbf{H}}_j}^\perp)^H = \mathbf{\Pi}_{\tilde{\mathbf{H}}_j}^\perp$, is used in Step (a) in (9).

A. Intra-Group Beam Design and the Corresponding Rates

In this subsection, we consider intra-group beam vector design for the mixture transceiver architecture and analyze the achievable rates of the intra-group processing. First, consider each group \mathcal{G}_j with one user. In this case, the received signal (9) reduces to

$$y_1^{(j)} = \left(\mathbf{\Pi}_{\tilde{\mathbf{H}}_j}^\perp \mathbf{h}_1^{(j)} \right)^H \sqrt{p_1^{(j)}} \mathbf{w}_1^{(j)} s_1^{(j)} + n_1^{(j)}, \quad |\mathcal{G}_j| = 1, \quad (11)$$

and the design of the intra-group beam vector $\mathbf{w}_1^{(j)}$ is simple. The optimal intra-group beam vector $\mathbf{w}_1^{(j)*}$ is the MRT beam matched to the projected effective channel vector $\mathbf{\Pi}_{\tilde{\mathbf{H}}_j}^\perp \mathbf{h}_1^{(j)}$, i.e., $\sqrt{p_1^{(j)}} \mathbf{w}_1^{(j)*} = \sqrt{P_t/K} \mathbf{\Pi}_{\tilde{\mathbf{H}}_j}^\perp \mathbf{h}_1^{(j)} / \|\mathbf{\Pi}_{\tilde{\mathbf{H}}_j}^\perp \mathbf{h}_1^{(j)}\|$. In this case, the optimal beam vector is equivalent to the ZF-beamforming vector with power P_t/K .

Next, consider the intra-group beam design for each group with more than one user. As aforementioned, we apply superposition coding and SIC in this case. Suppose that group \mathcal{G}_j consists of L users ($L > 1$). Then, with the group index (j) omitted for convenience, the received signal for User i , $i = 1, \dots, L$, in group \mathcal{G}_j is given by

$$y_i = \mathbf{g}_i^H \left(\sum_{i=1}^L \sqrt{p_i} \mathbf{w}_i s_i \right) + n_i, \quad i = 1 \dots, L, \quad (12)$$

where $\sum_{i=1}^L p_i \leq P$ with P being the total group power allocated to group \mathcal{G}_j (i.e., $P = L \times P_t/K$),

and \mathbf{g}_i is the projected effective channel of User i given by

$$\mathbf{g}_i = \mathbf{\Pi}_{\tilde{\mathbf{H}}_j}^\perp \mathbf{h}_i^{(j)}, \quad i = 1, \dots, L. \quad (13)$$

We assume that the intra-group beam vector \mathbf{w}_i is designed based on the projected effective channels $\mathbf{g}_1, \dots, \mathbf{g}_L$. Then, the feasible set for intra-group beam vector \mathbf{w}_i is given by $\mathcal{W} := \{\mathbf{w} \mid \|\mathbf{w}\|^2 \leq 1\}$ from the fact that the beam design space for \mathbf{w}_i is the linear subspace spanned by $\{\mathbf{g}_1, \dots, \mathbf{g}_L\}$. (The beam component not in the subspace spanned by $\{\mathbf{g}_1, \dots, \mathbf{g}_L\}$ does not affect the signal or the interference. Hence, it just wastes power.) Since $\mathbf{w}_i \in \mathcal{C}([\mathbf{g}_1, \dots, \mathbf{g}_L])$, we have $\mathbf{w}_i \in \mathcal{C}^\perp(\tilde{\mathbf{H}}_j)$ by (13) and hence for the actual beam power constraint $\|\mathbf{\Pi}^{(j)} \mathbf{w}_i\|^2 \leq 1$, we have $\|\mathbf{\Pi}^{(j)} \mathbf{w}_i\|^2 = \|\mathbf{\Pi}_{\tilde{\mathbf{H}}_j}^\perp \mathbf{w}_i\|^2 = \|\mathbf{w}_i\|^2 \leq 1$ in this case. So, we have the feasible set \mathcal{W} for \mathbf{w}_i .

Note that with inter-group ZF beamforming, the intra-group signal model is separated from group to group based on the projected effective channels, and the system model (12) is a conventional MISO BC with L -user superposition coding beamforming. For superposition coding and SIC, we assume that the in-group users are ordered according to their channel norms as $\|\mathbf{g}_1\|^2 \geq \|\mathbf{g}_2\|^2 \geq \dots \geq \|\mathbf{g}_L\|^2$. With this assumption, SIC at the in-group receivers is applied such that User i decodes and cancels the interference from Users $L, L-1, \dots, i+1$ sequentially.* (Note that since User i has a better channel than Users $L, L-1, \dots, i+1$, User i can decode the messages intended for Users $L, L-1, \dots, i+1$.) Then, the rates of the in-group users can be expressed as

$$R_1 = \log_2(1 + p_1 |\mathbf{g}_1^H \mathbf{w}_1|^2), \quad R_i = \log_2(1 + \min\{\text{SINR}_1^i, \dots, \text{SINR}_i^i\}), \quad i = 2, \dots, L, \quad (14)$$

where SINR_j^i is the SINR when User j decodes the message intended for User i , given by

$$\text{SINR}_j^i = \frac{p_i |\mathbf{g}_j^H \mathbf{w}_i|^2}{\sum_{m=1}^{i-1} p_m |\mathbf{g}_j^H \mathbf{w}_m|^2 + 1} \quad (15)$$

The achievable rate region \mathcal{R} of the MISO BC with superposition coding and SIC decoding is defined as the union of achievable rate-tuples:

$$\mathcal{R} := \bigcup_{\substack{(\mathbf{w}_1, \dots, \mathbf{w}_L) \in \mathcal{W}^L \\ (p_1, \dots, p_L) | p_i > 0, \forall i, \sum_{i=1}^L p_i = P}} (R_1, R_2, \dots, R_L), \quad (16)$$

where (R_1, \dots, R_L) is from (14). The Pareto boundary of the region \mathcal{R} is the outer boundary of

*The considered decoding order may not be optimal if we consider the design of $\{\mathbf{w}_i\}$ but is sufficient for our purpose of analytic derivation of the diversity order of the mixture transceiver architecture.

\mathcal{R} and can be obtained by maximizing R_L for each feasible target rate-tuple $(R_1^*, \dots, R_{L-1}^*)$. The maximization problem for given $(R_1^*, \dots, R_{L-1}^*)$ can be solved by a convex programming approach based on reformulation [18] and the convex concave procedure (CCP) [19]. However, difficulty lies in knowing the feasible target rate-tuple set for the MISO BC with superposition coding and SIC since the rates depend on the beam vectors and channel vectors of all in-group users, although some induction approach for this was proposed in [20]. The difficulty to find the feasible rate tuple for Users $1, \dots, L-1$ can be circumvented by formulating the problem as weighted sum rate maximization based on the rate-profile approach [21]. However, the existing algorithms for the Pareto-optimal design problem numerically provide rates based on numerically obtained beam vectors. Hence, these existing design algorithms do not provide closed-form rate expressions for general MISO BCs with superposition coding and SIC decoding which is necessary for our analytical derivation of the diversity order. In order to obtain desired closed-form expressions for the achievable rates of the MISO BC with superposition coding and SIC decoding, we consider beam design under the following constraint:

$$\begin{aligned} \mathbf{w}_1 &= \mathbf{w}_2 = \dots = \mathbf{w}_L = \mathbf{w}, \quad \|\mathbf{w}\|^2 \leq 1, \text{ i.e. } \mathbf{w} \in \mathcal{W} \\ p_i &= \delta_i P, \quad i = 1, 2, \dots, L, \end{aligned} \quad (17)$$

where $(\delta_1, \dots, \delta_L)$ is a power ratio-tuple out of the feasible power ratio-tuple set $\mathcal{D} := \{(\delta_1, \dots, \delta_L) \mid \delta_i \geq 0 \forall i, \sum_{i=1}^L \delta_i = 1\}$. Here, δ_i is the ratio of the total group power P to the power allocated to User i , i.e., $p_i = \delta_i P$ is assigned to User i . Note that the constraint (17) satisfies the original beam design constraint in (16). Based on the restricted constraint (17), the following proposition provides simple closed-form lower bounds on the achievable rates for the MISO BC with superposition coding and SIC:

Proposition 1: In the MISO BC (12) with L users adopting superposition coding and SIC decoding with channel vectors $\mathbf{g}_1, \dots, \mathbf{g}_L$ with ordering $\|\mathbf{g}_1\|^2 \geq \|\mathbf{g}_2\|^2 \geq \dots \geq \|\mathbf{g}_L\|^2$ and total group power P , for an arbitrary given power ratio-tuple $(\delta_1, \dots, \delta_L)$ out of the feasible power ratio-tuple set \mathcal{D} , the achievable rates (R_1, R_2, \dots, R_L) are lower bounded as

$$R_1 \geq \log_2 \left(1 + \frac{1}{c} \delta_1 \|\mathbf{g}_1\|^2 P \right) \quad (18)$$

$$R_i \geq \log_2 \left(1 + \frac{\delta_i}{\sum_{m=1}^{i-1} \delta_m} \frac{1}{1 + \left(\frac{1}{c} \|\mathbf{g}_i\|^2 \sum_{m=1}^{i-1} \delta_m P \right)^{-1}} \right), \quad i = 2, \dots, L, \quad (19)$$

where the constant c is given by

$$c = \begin{cases} L & \text{if, } L \leq 3, \\ 8L^2 & \text{if, } L > 3. \end{cases} \quad (20)$$

Proof: See Appendix A.

Note that the power ratio-tuple set \mathcal{D} does not depend on the beam vectors and the channel vectors, and it is just a simplex. Thus, the rate lower bounds (18) and (19) with sweeping $(\delta_1, \dots, \delta_L)$ within \mathcal{D} yield an inner region of the achievable rate region \mathcal{R} defined in (16).

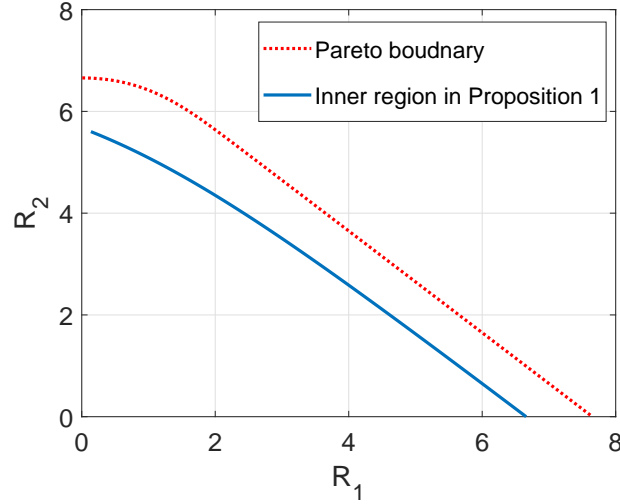


Fig. 1: Rate region: Pareto-boundary versus Proposition 1 ($K = 2$ with 4×1 MISO)

The rate lower bound in Proposition 1 was evaluated and compared with the Pareto-boundary obtained from (16) for an example case of a MISO BC of two users with SIC. The system setup is as follows: It was a MISO BC with four transmit antennas and one receive antenna, $10 \log_{10} P/1 = 10$, $\|\mathbf{g}_1\|^2 = 20$, $\|\mathbf{g}_2\|^2 = 10$, and $|\mathbf{g}_1^H \mathbf{g}_2|^2 / (\|\mathbf{g}_1\|^2 \|\mathbf{g}_2\|^2) = 0.5$, where \mathbf{g}_1 is the 4×1 channel vector of the strong user and \mathbf{g}_2 is the 4×1 channel vector of the weak user. The rate region is shown in Fig. 1. It is seen that the inner rate region by Proposition 1 is not very close to the Pareto-boundary, but it still achieves quite a good portion of the Pareto-region. The key point in the derived lower bounds (18) and (19) on the achievable rates (R_1, \dots, R_L) is that *the lower bound on the rate R_i of User i in the superposition-and-SIC group is expressed only in terms of User i 's channel norm square $\|\mathbf{g}_i\|^2$ and the power distribution factors $(\delta_1, \dots, \delta_L)$* . This enables us to analyze the distribution of R_i via the distribution of $\|\mathbf{g}_i\|^2$ and to derive the diversity order of the mixture scheme in Section IV.

B. Adaptive User Grouping

Now, we consider user grouping, which should be done properly for good diversity performance of the mixture transceiver architecture. Since we apply inter-group ZF beamforming, a level of orthogonality across the constructed groups is required to guarantee high reliability, as discussed in Section II-B. Note that the channel orthogonality among the users within a group is not required since superposition coding and SIC are applied to the users in each group. There can exist many user grouping methods that guarantee certain orthogonality among the constructed groups. In this section, we provide one example for such user grouping. The main difference between our user grouping method and several previous user grouping methods proposed for NOMA [14], [20], [22] is that the number of groups and the number of members in each group are not predetermined and the angle between the channel subspaces of any two user groups is not less than a certain threshold in our user grouping method, whereas the number of groups and the number of members in each group are predetermined and fixed for the previous methods [14], [20], [22]. This angle property is necessary for derivation of the diversity order of the mixture architecture.

To measure the orthogonality across groups, we define a new subspace angle metric $\theta(\cdot, \cdot)$, which captures the angle between the subspaces $\mathcal{C}(\mathbf{A})$ and $\mathcal{C}(\mathbf{B})$ spanned by the columns of matrices \mathbf{A} and \mathbf{B} as

$$\theta(\mathbf{A}, \mathbf{B}) := \begin{cases} \max(\{\phi(\mathbf{A}, \mathbf{b}_i), \forall i\} \cup \{\phi(\mathbf{B}, \mathbf{a}_j), \forall j\}), & \text{if } \mathbf{A} \text{ and } \mathbf{B} \text{ are non-empty matrices} \\ 0, & \text{if } \mathbf{A} \text{ or } \mathbf{B} \text{ is an empty matrix,} \end{cases} \quad (21)$$

where \mathbf{a}_i is the i -th column of \mathbf{A} , \mathbf{b}_j is the j -th column of \mathbf{B} , and $\phi(\cdot, \cdot)$ is another newly-defined angle metric which captures the angle between the vector \mathbf{b} and the subspace $\mathcal{C}(\mathbf{A})$, defined as

$$\phi(\mathbf{A}, \mathbf{b}) := \frac{\|\mathbf{A}(\mathbf{A}^H \mathbf{A})^{-1} \mathbf{A}^H \mathbf{b}\|^2}{\|\mathbf{b}\|^2}. \quad (22)$$

In case of $\mathbf{A} = [\mathbf{a}]$ is a vector, ϕ reduces to the square of the angle cosine of two vectors \mathbf{a} and \mathbf{b} :

$$\phi(\mathbf{a}, \mathbf{b}) = \frac{|\mathbf{a}^H \mathbf{b}|^2}{\|\mathbf{a}\|^2 \|\mathbf{b}\|^2} = \cos^2 \angle(\mathbf{a}, \mathbf{b}) \in [0, 1]. \quad (23)$$

When $\mathbf{B} = [\mathbf{b}]$ in (21) is a vector, $\theta(\mathbf{A}, \mathbf{b})$ simply reduces to $\phi(\mathbf{A}, \mathbf{b})$ because $\phi(\mathbf{A}, \mathbf{b}) \geq \phi(\mathbf{b}, \mathbf{a}_j)$ for all j , i.e., the angle between \mathbf{b} and $\mathcal{C}(\mathbf{A})$ is smaller than or equal to the angle between \mathbf{b} and individual column \mathbf{a}_j of \mathbf{A} , as illustrated in Fig. 2(a). When $\theta = 0$, two subspaces $\mathcal{C}(\mathbf{A})$ and $\mathcal{C}(\mathbf{B})$ are mutually orthogonal. When $\theta = 1$, on the other hand, there exists either at least a column of \mathbf{A} contained in $\mathcal{C}(\mathbf{B})$ or at least a column of \mathbf{B} contained in $\mathcal{C}(\mathbf{A})$, and the two subspaces $\mathcal{C}(\mathbf{A})$ and $\mathcal{C}(\mathbf{B})$ are not separated.

The proposed user grouping algorithm based on $\theta(\cdot, \cdot)$ is presented in Algorithm 1. Before explaining

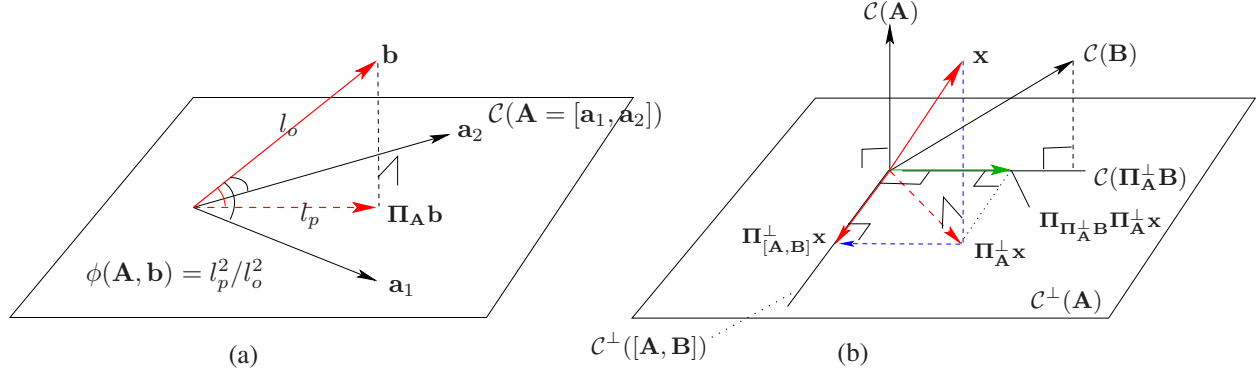


Fig. 2: (a) an illustration of $\phi(\mathbf{A}, \mathbf{b})$ and (b) an illustration of sequential orthogonal projection

the algorithm, we introduce a useful lemma regarding sequential orthogonal projection necessary to explain the algorithm.

Lemma 1: For a vector \mathbf{x} and matrices \mathbf{A} and \mathbf{B} such that $[\mathbf{A}, \mathbf{B}]$ is a tall matrix, the following equality holds: $\Pi_{[\mathbf{A}, \mathbf{B}]}^\perp \mathbf{x} = (\mathbf{I} - \Pi_{\Pi_{\mathbf{A}}^\perp \mathbf{B}}) \Pi_{\mathbf{A}}^\perp \mathbf{x} = \Pi_{\mathbf{A}}^\perp \mathbf{x} - \Pi_{\mathbf{A}}^\perp \mathbf{B} [(\Pi_{\mathbf{A}}^\perp \mathbf{B})^H \Pi_{\mathbf{A}}^\perp \mathbf{B}]^{-1} (\Pi_{\mathbf{A}}^\perp \mathbf{B})^H \Pi_{\mathbf{A}}^\perp \mathbf{x}$.

Proof: See Appendix B.

Lemma 1 states that the projection of \mathbf{x} onto the orthogonal space of $\mathcal{C}([\mathbf{A}, \mathbf{B}])$ can be accomplished in two steps first by projecting \mathbf{x} onto the orthogonal space of $\mathcal{C}(\mathbf{A})$ and then by projecting this projected vector onto the orthogonal space of $\mathcal{C}(\Pi_{\mathbf{A}}^\perp \mathbf{B})$ (not $\mathcal{C}(\mathbf{B})$), as illustrated in Fig. 2(b). By successively applying Lemma 1, we can obtain $\Pi_{[\mathbf{A}_1, \mathbf{A}_2, \dots, \mathbf{A}_n]}^\perp \mathbf{x}$ in a successive manner, where $[\mathbf{A}_1, \dots, \mathbf{A}_n]$ is a tall matrix. That is, we first project \mathbf{x} onto $\mathcal{C}^\perp(\mathbf{A}_1)$ to obtain $\Pi_{\mathbf{A}_1}^\perp \mathbf{x}$, and project the subspace matrices $\mathbf{A}_2, \mathbf{A}_3, \dots, \mathbf{A}_n$ onto $\mathcal{C}^\perp(\mathbf{A}_1)$ to obtain $\Pi_{\mathbf{A}_1}^\perp \mathbf{A}_2, \Pi_{\mathbf{A}_1}^\perp \mathbf{A}_3, \dots, \Pi_{\mathbf{A}_1}^\perp \mathbf{A}_n$. Then, we project $\Pi_{\mathbf{A}_1}^\perp \mathbf{x}$ onto $\mathcal{C}^\perp(\Pi_{\mathbf{A}_1}^\perp \mathbf{A}_2)$ to obtain $(\mathbf{I} - \Pi_{\Pi_{\mathbf{A}_1}^\perp \mathbf{A}_2}) \Pi_{\mathbf{A}_1}^\perp \mathbf{x}$, and also project $\Pi_{\mathbf{A}_1}^\perp \mathbf{A}_3, \dots, \Pi_{\mathbf{A}_1}^\perp \mathbf{A}_n$ onto $\mathcal{C}^\perp(\Pi_{\mathbf{A}_1}^\perp \mathbf{A}_2)$ to obtain $(\mathbf{I} - \Pi_{\Pi_{\mathbf{A}_1}^\perp \mathbf{A}_2}) \Pi_{\mathbf{A}_1}^\perp \mathbf{A}_3, \dots, (\mathbf{I} - \Pi_{\Pi_{\mathbf{A}_1}^\perp \mathbf{A}_2}) \Pi_{\mathbf{A}_1}^\perp \mathbf{A}_n$. Then, we project $(\mathbf{I} - \Pi_{\Pi_{\mathbf{A}_1}^\perp \mathbf{A}_2}) \Pi_{\mathbf{A}_1}^\perp \mathbf{x}$ onto $\mathcal{C}^\perp((\mathbf{I} - \Pi_{\Pi_{\mathbf{A}_1}^\perp \mathbf{A}_2}) \Pi_{\mathbf{A}_1}^\perp \mathbf{A}_3)$, and project the remaining subspace matrices $(\mathbf{I} - \Pi_{\Pi_{\mathbf{A}_1}^\perp \mathbf{A}_2}) \Pi_{\mathbf{A}_1}^\perp \mathbf{A}_4, \dots, (\mathbf{I} - \Pi_{\Pi_{\mathbf{A}_1}^\perp \mathbf{A}_2}) \Pi_{\mathbf{A}_1}^\perp \mathbf{A}_n$ correspondingly. We continue this process until step n is reached. Then, this gives us $\Pi_{[\mathbf{A}_1, \mathbf{A}_2, \dots, \mathbf{A}_n]}^\perp \mathbf{x}$.

Algorithm 1 tries to find single-user groups first (line 6). If the algorithm cannot find any single-user group further, it increases the number of users in group to two (lines 17 and 18), and tries to find two-user groups. It continues this process until n_g becomes K (line 9). Suppose that no group is found up to $n_g = K - 1$. Then, at $n_g = K$, one argument in $\theta(\cdot, \cdot)$ in (24) becomes an empty matrix, θ becomes zero by the definition (21), and hence the condition (24) is satisfied. Thus, in this case the whole set $\{1, 2, \dots, K\}$ becomes a single group. Let us explain Algorithm 1 by using a specific example below:

Algorithm 1 : The Proposed User Grouping Algorithm

-
- 1: **Initialization:**
- 2: A threshold value $\theta^{th} \in (0, 1)$ is given.
- 3: Initially set $\mathbf{f}_1, \dots, \mathbf{f}_K$ as the actual channel vectors $\mathbf{h}_1, \dots, \mathbf{h}_K$ of the K users.
- 4: Set $\mathcal{K} \leftarrow \{1, \dots, K\}$ (initial candidate set)
- 5: Set $i_g \leftarrow 0$ (group index)
- 6: Set $n_g \leftarrow 1$ (number of users in group)
- 7: Set $\mathbf{F}_{\mathcal{K}} \leftarrow [\mathbf{f}_1, \dots, \mathbf{f}_K]$.
- 8: **Execution:**
- 9: **While** $n_g \leq K$
- 10: Find a group of users $\{u_1^*, \dots, u_{n_g}^*\}$ with cardinality n_g such that $\mathcal{C}(\mathbf{F}_{\{u_1^*, \dots, u_{n_g}^*\}})$ and $\mathcal{C}(\mathbf{F}_{\mathcal{K} \setminus \{u_1^*, \dots, u_{n_g}^*\}})$ satisfy
- $$\theta(\mathbf{F}_{\mathcal{K} \setminus \{u_1^*, \dots, u_{n_g}^*\}}, \mathbf{F}_{\{u_1^*, \dots, u_{n_g}^*\}}) \leq \theta^{th}. \quad (24)$$
- 11: **If** we find such a group of users $\{u_1^*, \dots, u_{n_g}^*\}$,
- 12: $i_g \leftarrow i_g + 1$ (increase the group index by one).
- 13: $\mathcal{G}_{i_g} \leftarrow \{u_1^*, \dots, u_{n_g}^*\}$ (construct one group).
- 14: $\mathcal{K} \leftarrow \mathcal{K} \setminus \{u_1^*, \dots, u_{n_g}^*\}$ (update \mathcal{K} by removing the selected users from the candidate set).
- 15: Update the vector \mathbf{f}_u as $\mathbf{f}_u \leftarrow (\mathbf{I} - \mathbf{F}_{\mathcal{G}_{i_g}} (\mathbf{F}_{\mathcal{G}_{i_g}}^H \mathbf{F}_{\mathcal{G}_{i_g}})^{-1} \mathbf{F}_{\mathcal{G}_{i_g}}^H) \mathbf{f}_u, \forall u \in \text{updated } \mathcal{K}$
- 16: Construct new $\mathbf{F}_{\mathcal{K}}$ with the updated $\mathbf{f}_u, \forall u \in \text{updated } \mathcal{K}$.
- 17: **Else**
- 18: $n_g \leftarrow n_g + 1$
- 19: **Endif**
- 20: **Endwhile**
- 21: $N_g \leftarrow i_g$.
- 22: (Throughout the algorithm, $\mathbf{F}_{\mathcal{S}}$ means the submatrix of current $\mathbf{F}_{\mathcal{K}}$ composed of $\{\text{current } \mathbf{f}_u, \forall u \in \mathcal{S} \subset \mathcal{K}\}$.)
-

Example 1: Suppose that initial $\mathcal{K} = \{1, 2, 3, 4, 5, 6, 7\}$ and suppose that initially user 1 satisfies $\theta([\mathbf{h}_2, \dots, \mathbf{h}_7], \mathbf{h}_1) \leq \theta^{th}$. Then, we update $\mathcal{G}_1 = \{1\}$ (line 13) and $\mathcal{K} = \{2, 3, 4, 5, 6, 7\}$ (line 14), and project the channel vectors $\mathbf{h}_2, \dots, \mathbf{h}_7$ onto $\mathcal{C}^\perp([\mathbf{h}_1])$ to obtain the projected channel vectors $\Pi_{\mathbf{h}_1}^\perp \mathbf{h}_2, \dots, \Pi_{\mathbf{h}_1}^\perp \mathbf{h}_7$ (line 15). Next, suppose that $\theta([\Pi_{\mathbf{h}_1}^\perp \mathbf{h}_3, \dots, \Pi_{\mathbf{h}_1}^\perp \mathbf{h}_7], \Pi_{\mathbf{h}_1}^\perp \mathbf{h}_2) \leq \theta^{th}$. (Note that at this point we compute $\theta(\cdot, \cdot)$ using the *projected* channels (lines 15 and 16).) Then, we update $\mathcal{G}_2 = \{2\}$ and $\mathcal{K} = \{3, 4, 5, 6, 7\}$ and project $\Pi_{\mathbf{h}_1}^\perp \mathbf{h}_3, \dots, \Pi_{\mathbf{h}_1}^\perp \mathbf{h}_7$ onto $\mathcal{C}^\perp(\Pi_{\mathbf{h}_1}^\perp \mathbf{h}_2)$ to obtain the further projected channels $(\mathbf{I} - \Pi_{\Pi_{\mathbf{h}_1}^\perp \mathbf{h}_2}) \Pi_{\mathbf{h}_1}^\perp \mathbf{h}_3, \dots, (\mathbf{I} - \Pi_{\Pi_{\mathbf{h}_1}^\perp \mathbf{h}_2}) \Pi_{\mathbf{h}_1}^\perp \mathbf{h}_7$. Now, suppose that we cannot find a single-user group further and that at $n_g = 2$ only one pair of users $\{3, 4\}$ satisfies $\theta([\Pi_{\Pi_{\mathbf{h}_1}^\perp \mathbf{h}_2}^\perp \Pi_{\mathbf{h}_1}^\perp \mathbf{h}_5, \dots, (\mathbf{I} - \Pi_{\Pi_{\mathbf{h}_1}^\perp \mathbf{h}_2}) \Pi_{\mathbf{h}_1}^\perp \mathbf{h}_7]) \leq \theta^{th}$.

$\Pi_{\Pi_{\mathbf{h}_1}^\perp \mathbf{h}_2} \Pi_{\mathbf{h}_1}^\perp \mathbf{h}_7]$, $[(\mathbf{I} - \Pi_{\Pi_{\mathbf{h}_1}^\perp \mathbf{h}_2}) \Pi_{\mathbf{h}_1}^\perp \mathbf{h}_3, (\mathbf{I} - \Pi_{\Pi_{\mathbf{h}_1}^\perp \mathbf{h}_2}) \Pi_{\mathbf{h}_1}^\perp \mathbf{h}_4]) \leq \theta^{th}$. Then, we update $\mathcal{G}_3 = \{3, 4\}$ and $\mathcal{K} = \{5, 6, 7\}$, and the further projected channels for users $\{5, 6, 7\}$ are obtained by projecting $(\mathbf{I} - \Pi_{\Pi_{\mathbf{h}_1}^\perp \mathbf{h}_2}) \Pi_{\mathbf{h}_1}^\perp \mathbf{h}_5, \dots, (\mathbf{I} - \Pi_{\Pi_{\mathbf{h}_1}^\perp \mathbf{h}_2}) \Pi_{\mathbf{h}_1}^\perp \mathbf{h}_7$ onto $\mathcal{C}^\perp([(\mathbf{I} - \Pi_{\Pi_{\mathbf{h}_1}^\perp \mathbf{h}_2}) \Pi_{\mathbf{h}_1}^\perp \mathbf{h}_3, (\mathbf{I} - \Pi_{\Pi_{\mathbf{h}_1}^\perp \mathbf{h}_2}) \Pi_{\mathbf{h}_1}^\perp \mathbf{h}_4])$. These final projected channels for users $\{5, 6, 7\}$ are the same as the ZF projected channels $\Pi_{[\mathbf{h}_1, \dots, \mathbf{h}_4]}^\perp \mathbf{h}_5, \dots, \Pi_{[\mathbf{h}_1, \dots, \mathbf{h}_4]}^\perp \mathbf{h}_7$ by Lemma 1. At the next iteration, n_g becomes 3 since we assumed that there is no further two-user group; one argument of $\theta(\cdot, \cdot)$ becomes an empty matrix since $\mathcal{K} = \{5, 6, 7\}$ and $n_g = 3$; hence $\mathcal{G}_4 = \{5, 6, 7\}$; no user is left in the candidate set \mathcal{K} after update (line 14); no further channel projection in line 15 occurs since updated $\mathcal{K} = \emptyset$; and the algorithm stops.

Now, let us consider the norm property of the projected ZF channels associated with the constructed groups in the example, which is the key aspect of the proposed user grouping algorithm. Consider user 1 in firstly-constructed \mathcal{G}_1 . Since $\theta([\mathbf{h}_2, \dots, \mathbf{h}_7], \mathbf{h}_1) \leq \theta^{th}$, by the definition of $\theta(\cdot, \cdot)$ in (21), we have

$$\phi(\tilde{\mathbf{H}}_1 = [\mathbf{h}_2, \dots, \mathbf{h}_7], \mathbf{h}_1) = \frac{\|\tilde{\mathbf{H}}_1(\tilde{\mathbf{H}}_1^H \tilde{\mathbf{H}}_1)^{-1} \tilde{\mathbf{H}}_1^H \mathbf{h}_1\|^2}{\|\mathbf{h}_1\|^2} \leq \theta^{th} \quad (25)$$

Hence, we have

$$\begin{aligned} \|\Pi_{\tilde{\mathbf{H}}_1}^\perp \mathbf{h}_1\|^2 &= \|(\mathbf{I} - \tilde{\mathbf{H}}_1(\tilde{\mathbf{H}}_1^H \tilde{\mathbf{H}}_1)^{-1} \tilde{\mathbf{H}}_1^H) \mathbf{h}_1\|^2 \\ &= (1 - \phi(\tilde{\mathbf{H}}_1, \mathbf{h}_1)) \|\mathbf{h}_1\|^2 \text{ by the Pythagorean theorem} \\ &\geq (1 - \theta^{th}) \|\mathbf{h}_1\|^2. \end{aligned}$$

Next, consider the norm of the ZF effective channel for User 2 in \mathcal{G}_2 . Due to the construction of \mathcal{G}_1 based on (25), \mathbf{h}_1 and \mathbf{h}_2 satisfy the following:

$$\begin{aligned} \|\Pi_{\mathbf{h}_1}^\perp \mathbf{h}_2\|^2 &= (1 - \phi(\mathbf{h}_1, \mathbf{h}_2)) \|\mathbf{h}_2\|^2 \\ &\geq (1 - \phi(\tilde{\mathbf{H}}_1, \mathbf{h}_1)) \|\mathbf{h}_2\|^2, \text{ since } \tilde{\mathbf{H}}_1 \text{ includes } \mathbf{h}_2 \\ &\geq (1 - \theta^{th}) \|\mathbf{h}_2\|^2. \end{aligned} \quad (26)$$

By Lemma 1, $\Pi_{[\mathbf{h}_1, \mathbf{h}_3, \dots, \mathbf{h}_7]}^\perp \mathbf{h}_2$ can be obtained by sequential orthogonal projection as

$$\Pi_{[\mathbf{h}_1, \mathbf{h}_3, \dots, \mathbf{h}_7]}^\perp \mathbf{h}_2 = (\mathbf{I} - \Pi_{[\Pi_{\mathbf{h}_1}^\perp \mathbf{h}_3, \dots, \Pi_{\mathbf{h}_1}^\perp \mathbf{h}_7]}) \Pi_{\mathbf{h}_1}^\perp \mathbf{h}_2,$$

but \mathcal{G}_2 was constructed such that $\Pi_{\mathbf{h}_1}^\perp \mathbf{h}_2$ and $[\Pi_{\mathbf{h}_1}^\perp \mathbf{h}_3, \dots, \Pi_{\mathbf{h}_1}^\perp \mathbf{h}_7]$ satisfy the threshold θ^{th} requirement.

Combining this fact and (26), we have

$$\|\Pi_{[\mathbf{h}_1, \mathbf{h}_3, \dots, \mathbf{h}_7]}^\perp \mathbf{h}_2\|^2 \geq (1 - \theta^{th})^2 \|\mathbf{h}_2\|^2.$$

Then, consider User 3 in $\mathcal{G}_3 = \{3, 4\}$. (The same applies to User 4 in \mathcal{G}_3 .) By Lemma 1, we have

$$\Pi_{[\mathbf{h}_1, \mathbf{h}_2]}^\perp \mathbf{h}_3 = (\mathbf{I} - \Pi_{\Pi_{[\mathbf{h}_1, \mathbf{h}_2]}^\perp \mathbf{h}_2}) \Pi_{[\mathbf{h}_1, \mathbf{h}_2]}^\perp \mathbf{h}_3 \quad (27)$$

$$\Pi_{[\mathbf{h}_1, \mathbf{h}_2, \mathbf{h}_5, \mathbf{h}_6, \mathbf{h}_7]}^\perp \mathbf{h}_3 = (\mathbf{I} - \Pi_{[\Pi_{[\mathbf{h}_1, \mathbf{h}_2]}^\perp \mathbf{h}_5, \Pi_{[\mathbf{h}_1, \mathbf{h}_2]}^\perp \mathbf{h}_6, \Pi_{[\mathbf{h}_1, \mathbf{h}_2]}^\perp \mathbf{h}_7]}) \Pi_{[\mathbf{h}_1, \mathbf{h}_2]}^\perp \mathbf{h}_3. \quad (28)$$

In (27), $\mathcal{G}_1 = \{1\}$ was constructed such that \mathbf{h}_1 and \mathbf{h}_3 satisfy the angle constraint, and $\mathcal{G}_2 = \{2\}$ was constructed such that $\Pi_{[\mathbf{h}_1]}^\perp \mathbf{h}_2$ and $\Pi_{[\mathbf{h}_1]}^\perp \mathbf{h}_3$ satisfy the angle constraint. Hence, we have $\|\Pi_{[\mathbf{h}_1]}^\perp \mathbf{h}_3\|^2 \geq (1 - \theta^{th})^2 \|\mathbf{h}_3\|^2$. Furthermore, in (28), $\mathcal{G}_3 = \{3, 4\}$ was constructed such that $[\Pi_{[\mathbf{h}_1, \mathbf{h}_2]}^\perp \mathbf{h}_3, \Pi_{[\mathbf{h}_1, \mathbf{h}_2]}^\perp \mathbf{h}_4]$ and the remaining $[\Pi_{[\mathbf{h}_1, \mathbf{h}_2]}^\perp \mathbf{h}_5, \Pi_{[\mathbf{h}_1, \mathbf{h}_2]}^\perp \mathbf{h}_6, \Pi_{[\mathbf{h}_1, \mathbf{h}_2]}^\perp \mathbf{h}_7]$ satisfy the angle constraint. Combining these facts, we have

$$\|\Pi_{[\mathbf{h}_1, \mathbf{h}_2, \mathbf{h}_5, \mathbf{h}_6, \mathbf{h}_7]}^\perp \mathbf{h}_k\|^2 \geq (1 - \theta^{th})^3 \|\mathbf{h}_k\|^2, \quad k = 3, 4. \quad (29)$$

Finally, consider the norm of the ZF effective channels $\Pi_{[\mathbf{h}_1, \dots, \mathbf{h}_4]}^\perp \mathbf{h}_5, \dots, \Pi_{[\mathbf{h}_1, \dots, \mathbf{h}_4]}^\perp \mathbf{h}_7$ of the last group $\mathcal{G}_4 = \{5, 6, 7\}$. These vectors are obtained by three sequential orthogonal projections based on Lemma 1, and at each projection stage the threshold θ^{th} was kept for group splitting. Hence, we have

$$\|\Pi_{[\mathbf{h}_1, \dots, \mathbf{h}_4]}^\perp \mathbf{h}_k\|^2 \geq (1 - \theta^{th})^3 \|\mathbf{h}_k\|^2, \quad k = 5, 6, 7.$$

Note that in general the proposed user grouping algorithm satisfies the following norm reduction property for the ZF effective channels:

$$\|\mathbf{g}_i^{(j)}\|^2 = \|\Pi_{\mathbf{H}_j}^\perp \mathbf{h}_i^{(j)}\|^2 \geq (1 - \theta^{th})^{N_g - 1} \|\mathbf{h}_i^{(j)}\|^2, \quad (30)$$

where $\Pi_{\mathbf{H}_j}^\perp$ is the ZF projection matrix for group \mathcal{G}_j , $\mathbf{h}_i^{(j)}$ is the channel vector of User i in group \mathcal{G}_j , and N_g is the number of constructed groups, which is bounded by K . Since the number of antennas N and the number of users K ($\leq N$) are fixed in our MISO BC model with superposition coding and SIC, the lower bound $(1 - \theta^{th})^{K-1} \in (0, 1)$ of $(1 - \theta^{th})^{N_g-1}$ is a constant.

Now, let us define a useful quantity for further exposition: We define the degrees of freedom of a fading channel \mathbf{h} as

$$d := \lim_{x \rightarrow 0} \frac{\log \Pr(\|\mathbf{h}\|^2 \leq x)}{\log x}. \quad (31)$$

This quantity captures the behavior of the tail probability of the random variable $\|\mathbf{h}\|^2$ in its lower tail,

and the degrees of freedom d for \mathbf{h} means that $\Pr(\|\mathbf{h}\|^2 \leq x)$ behaves as $x^d + o(x^d)$, as $x \rightarrow 0$. This quantity is directly related to the diversity order of the SISO communication channel with the channel gain $\|\mathbf{h}\|$. For example, a Rayleigh fading channel $\mathbf{h} \sim \mathcal{C}(\mathbf{0}, 2\mathbf{I}_N)$ has the degrees of freedom N since

$$\Pr(\|\mathbf{h}\|^2 \leq x) = \int_0^x f_{\|\mathbf{h}\|^2}(z) dz = \frac{1}{2^N N!} x^N + o(x^N), \text{ as } x \rightarrow 0 \quad (32)$$

and $\lim_{x \rightarrow 0} \frac{\log \Pr(\|\mathbf{h}\|^2 \leq x)}{\log x} = N$, where $f_{\|\mathbf{h}\|^2}(z) dz$ is given in (5). Finally, we provide the main statement of this subsection regarding the degrees of freedom of the ZF effective channels associated with the proposed grouping method in the following proposition:

Proposition 2: With the mixture transceiver architecture and the user grouping method in Algorithm 1, the projected effective channel $\mathbf{g}_j^{(i)} = \mathbf{\Pi}_{\mathbf{H}_j}^\perp \mathbf{h}_i^{(j)}$ in (9) resulting from inter-group ZF beamforming has the same degrees of freedom as the original channel $\mathbf{h}_i^{(j)}$, i.e.,

$$\lim_{x \rightarrow 0} \frac{\log \Pr(\|\mathbf{g}_i^{(j)}\|^2 \leq x)}{\log x} = \lim_{x \rightarrow 0} \frac{\log \Pr(\|\mathbf{h}_i^{(j)}\|^2 \leq x)}{\log x}, \quad \forall i, j. \quad (33)$$

Proof: See Appendix C.

Complexity of Algorithm 1: Note that in the worst case the number of group searches is given by $K + \binom{K}{2} + \binom{K}{3} + \dots + \binom{K}{K}$, which scales as $K^{K/2}$. For each group search, we need to compute $\theta(\cdot, \cdot)$ in (24), which requires inversion of $K \times K$ matrices in the worst case (see (24) and the term $(\mathbf{A}^H \mathbf{A})^{-1}$ in (22)). Thus, Algorithm 1 is not scalable for large K . Nevertheless, the algorithm is devised to prove the diversity-order optimality of the mixture architecture in this paper. Invention of more efficient user grouping algorithms for the mixture architecture for MISO BCs is a future work. For one possible idea for polynomial complexity, please see Appendix E.

SIC Complexity: Since in the proposed adaptive user grouping, each group can have one to K members, it is required that each receiver be able to handle SIC of $K - 1$ users in the worst case. SIC for a general number of users has been investigated extensively for code-division multiple access systems [23].

IV. OUTAGE ANALYSIS AND DIVERSITY ORDER OF THE MIXTURE SCHEME

In this section, we present our main result regarding the diversity order of the mixture transceiver architecture for MISO BCs.

Theorem 1: For the Gaussian MISO BC with N transmit antennas and K single-antenna users with independent Rayleigh fading described in Section II-A, let the channels be ordered as $\|\mathbf{h}_1\|^2 \geq \|\mathbf{h}_2\|^2 \dots \geq \|\mathbf{h}_K\|^2$ and let the k -th user be the user with the k -th largest channel norm. Then, the diversity order for

the k -th user achievable by the mixture transceiver architecture with proper user grouping is given by

$$D_k = N \times (K - k + 1). \quad (34)$$

Here, the diversity order is defined as $D_k := \lim_{P_t \rightarrow \infty} -\frac{\log \Pr\{R_k < R^{th}\}}{\log P_t}$, where R_k is the rate of the k -th user and R^{th} is a rate threshold. Note that $P_t \rightarrow \infty$ is equivalent to $\text{SNR} = P_t/\sigma^2 \rightarrow \infty$ since we set the noise variance $\sigma^2 = 1$ for simplicity.

Proof: For user grouping of the mixture architecture we adopt Algorithm 1. The diversity provided by such a grouping will provide an achievable bound for the diversity as claimed in the theorem. Proof is based on Propositions 1 and 2. In proof, we consider not only the distribution of the channel norm itself but also the order statistics resulting from the channel norm ordering. With the descending channel ordering $\|\mathbf{h}_1\|^2 \geq \|\mathbf{h}_2\|^2 \cdots \geq \|\mathbf{h}_K\|^2$, the pdf of the k -th channel norm square is given by order statistics as

$$f_{\|\mathbf{h}_k\|^2}(x) = \frac{K!}{(k-1)!(K-k)!} [F_{\|\mathbf{h}\|^2}(x)]^{K-k} [1 - F_{\|\mathbf{h}\|^2}(x)]^{k-1} f_{\|\mathbf{h}\|^2}(x) \quad (35)$$

where $f_{\|\mathbf{h}\|^2}(\cdot)$ and $F_{\|\mathbf{h}\|^2}$ are the pdf and cumulative distribution function (cdf) of chi-square distribution with degree of freedom $2N$:

$$f_{\|\mathbf{h}\|^2}(x) = \frac{1}{2^N (N-1)!} x^{N-1} e^{-x/2} = \frac{1}{2^N N!} x^{N-1} + o(x^{N-1}), \quad \text{as } x \rightarrow 0 \quad (36)$$

$$F_{\|\mathbf{h}\|^2}(x) = \frac{1}{2^N N!} x^N + o(x^N), \quad \text{as } x \rightarrow 0. \quad (37)$$

Hence, we have for the k -th largest channel norm square $\|\mathbf{h}_k\|^2$

$$f_{\|\mathbf{h}_k\|^2}(x) = c_k x^{N(K-k+1)-1} + o(x^{N(K-k+1)-1}), \quad \text{as } x \rightarrow 0, \quad (38)$$

and thus

$$\lim_{x \rightarrow 0} \frac{\log \Pr(\|\mathbf{h}_k\|^2 \leq x)}{\log x} = N(K - k + 1). \quad (39)$$

The outage probability of the k -th user is expressed as

$$\Pr(R_k < R^{th}) = \sum_{j=1}^{N_g} \left[\Pr(k \in \mathcal{G}_j) \cdot \Pr(R_k < R^{th} \mid k \in \mathcal{G}_j) \right] \quad (40)$$

$$\begin{aligned} &= \sum_{j=1}^{N_g} \left[\Pr(k \in \mathcal{G}_j) \cdot \left\{ \Pr(|\mathcal{G}_j| = 1 \mid k \in \mathcal{G}_j) \cdot \Pr(R_k < R^{th} \mid |\mathcal{G}_j| = 1, k \in \mathcal{G}_j) \right. \right. \\ &\quad \left. \left. + \Pr(|\mathcal{G}_j| \neq 1 \mid k \in \mathcal{G}_j) \cdot \Pr(R_k < R^{th} \mid |\mathcal{G}_j| \neq 1, k \in \mathcal{G}_j) \right\} \right]. \quad (41) \end{aligned}$$

i) Lower bound on the outage probability: We obtain a lower bound on the outage probability by considering only the event that the k -th user belongs to a group with cardinality one, i.e., the first term in the RHS of (41).

$$\begin{aligned}
\Pr(R_k < R^{th}) &\geq \sum_{j=1}^{N_g} \Pr(k \in \mathcal{G}_j) \cdot \Pr(|\mathcal{G}_j| = 1 \mid k \in \mathcal{G}_j) \cdot \Pr(R_k < R^{th} \mid |\mathcal{G}_j| = 1, k \in \mathcal{G}_j) \\
&= \sum_{j=1}^{N_g} \Pr(|\mathcal{G}_j| = 1, k \in \mathcal{G}_j) \cdot \Pr(R_k < R^{th} \mid |\mathcal{G}_j| = 1, k \in \mathcal{G}_j) \\
&= \sum_{j=1}^{N_g} \Pr(|\mathcal{G}_j| = 1, k \in \mathcal{G}_j) \cdot \Pr\left(\|\mathbf{\Pi}^{(j)} \mathbf{h}_k\|^2 < K \cdot (2^{R^{th}} - 1) \cdot P_t^{-1}\right), \tag{42}
\end{aligned}$$

where (42) holds due to the rate $R_k = \log(1 + P_t \|\mathbf{\Pi}^{(j)} \mathbf{h}_k\|^2 / K)$ for a single-user group based on (11) and the corresponding optimal beam. Then, we have

$$-D_k = \lim_{P_t \rightarrow \infty} \frac{\log \Pr(R_k < R^{th})}{\log P_t} \tag{43}$$

$$\geq \lim_{P_t \rightarrow \infty} \frac{\log \left(\sum_{j=1}^{N_g} \left[\Pr(|\mathcal{G}_j| = 1, k \in \mathcal{G}_j) \cdot \Pr\left(\|\mathbf{\Pi}^{(j)} \mathbf{h}_k\|^2 < K \cdot (2^{R^{th}} - 1) \cdot P_t^{-1}\right) \right] \right)}{\log P_t} \tag{44}$$

$$= \lim_{P_t^{-1} \rightarrow 0} \frac{\log \left(\sum_{j=1}^{N_g} \left[\Pr(|\mathcal{G}_j| = 1, k \in \mathcal{G}_j) \cdot \Pr\left(\|\mathbf{\Pi}^{(j)} \mathbf{h}_k\|^2 < K \cdot (2^{R^{th}} - 1) \cdot P_t^{-1}\right) \right] \right)}{-\log P_t^{-1}} \tag{45}$$

$$= -N(K - k + 1). \tag{46}$$

Here, (46) is valid because $\|\mathbf{h}_k\|^2$ has the channel order $N(K - k + 1)$ by (38) and (39); the projected effective channel $\|\mathbf{\Pi}^{(j)} \mathbf{h}_k\|^2$ has the same channel order as $\|\mathbf{h}_k\|^2$ by Proposition 2; and the linear combination of terms with the same order has the same order as each term. Note that $\Pr(|\mathcal{G}_j| = 1, k \in \mathcal{G}_j)$ depends only on the joint distribution of $(\mathbf{h}_1, \dots, \mathbf{h}_k)$ for the given user grouping algorithm not on the power P_t .

ii) Upper bound on the outage probability:

For the upper bound, we need to include the second term in the RHS of (41) in addition to the first term in the RHS of (41) considered in the lower bound. The second term in the RHS of (41) is given by

$$\sum_{j=1}^{N_g} \Pr(k \in \mathcal{G}_j) \cdot \Pr(|\mathcal{G}_j| \neq 1 \mid k \in \mathcal{G}_j) \cdot \Pr(R_k < R^{th} \mid |\mathcal{G}_j| \neq 1, k \in \mathcal{G}_j) \tag{47}$$

$$= \sum_{j=1}^{N_g} \Pr(|\mathcal{G}_j| \neq 1, k \in \mathcal{G}_j) \cdot \Pr(R_k < R^{th} \mid |\mathcal{G}_j| \neq 1, k \in \mathcal{G}_j) \tag{48}$$

$$= \sum_{j=1}^{N_g} \sum_{\ell=2}^K \Pr(|\mathcal{G}_j| = \ell, k \in \mathcal{G}_j) \cdot \underbrace{\Pr(R_k < R^{th} \mid |\mathcal{G}_j| = \ell, k \in \mathcal{G}_j)}_{(a)}. \quad (49)$$

Define the following notations:

$$E_{k,j,i} := \text{Event that the } k\text{-th user is the } i\text{-th largest channel norm user in } \mathcal{G}_j \quad (50)$$

$$P_{k,j,i} := \Pr(E_{k,j,i}). \quad (51)$$

With these notations, the term (a) in (49) can be rewritten as

$$\Pr(R_k < R^{th} \mid |\mathcal{G}_j| = \ell, k \in \mathcal{G}_j) = \sum_{i=1}^{\ell} P_{k,j,i} \cdot \Pr(R_k < R^{th} \mid |\mathcal{G}_j| = \ell, k \in \mathcal{G}_j, E_{k,j,i}), \quad (52)$$

where R_k conditioned on the joint event $(|\mathcal{G}_j| = \ell, k \in \mathcal{G}_j, E_{k,j,i})$ is lower bounded by Proposition 1 as

$$R_k \geq \begin{cases} \log_2 \left(1 + \frac{1}{c} \delta_1^{(j)} \|\mathbf{\Pi}^{(j)} \mathbf{h}_k\|^2 \frac{\ell P_t}{K} \right) & \text{if } i = 1 \\ \log_2 \left(1 + \frac{\delta_i^{(j)}}{\sum_{m=1}^{i-1} \delta_m^{(j)}} \frac{1}{1 + \left(\frac{1}{c} \|\mathbf{\Pi}^{(j)} \mathbf{h}_k\|^2 \sum_{m=1}^{i-1} \delta_m^{(j)} \frac{\ell P_t}{K} \right)^{-1}} \right) & \text{if } i = 2 \cdots \ell. \end{cases} \quad (53)$$

where c is given in (20), and $(\delta_1^{(j)}, \delta_2^{(j)}, \dots, \delta_{\ell}^{(j)})$ is the power ratio-tuple in group \mathcal{G}_j , i.e., power $\delta_i^{(j)} \ell P_t / K$ is assigned to User i in group \mathcal{G}_j . ($\ell P_t / K$ is the total group power for group \mathcal{G}_j with $|\mathcal{G}_j| = \ell$.) Therefore, the probability (52) is upper bounded as

$$\sum_{i=1}^{\ell} \left[P_{k,j,i} \cdot \Pr(R_k < R^{th} \mid |\mathcal{G}_j| = \ell, k \in \mathcal{G}_j, E_{k,j,i}) \right] \quad (54)$$

$$\begin{aligned} &\leq P_{k,j,1} \cdot \Pr \left(\log_2 \left(1 + \frac{1}{c} \delta_1^{(j)} \|\mathbf{\Pi}^{(j)} \mathbf{h}_k\|^2 \frac{\ell P_t}{K} \right) < R^{th} \right) \\ &\quad + \sum_{i=2}^{\ell} \left[P_{k,j,i} \cdot \Pr \left(\log_2 \left(1 + \frac{\delta_i^{(j)}}{\sum_{m=1}^{i-1} \delta_m^{(j)}} \frac{1}{1 + \left(\frac{1}{c} \|\mathbf{\Pi}^{(j)} \mathbf{h}_k\|^2 \sum_{m=1}^{i-1} \delta_m^{(j)} \ell P_t / K \right)^{-1}} \right) < R^{th} \right) \right] \end{aligned} \quad (55)$$

$$\begin{aligned} &= P_{k,j,1} \cdot \Pr \left(\|\mathbf{\Pi}^{(j)} \mathbf{h}_k\|^2 < (2^{R^{th}} - 1) \cdot \frac{c}{\delta_1^{(j)}} \cdot \frac{K}{\ell} P_t^{-1} \right) \\ &\quad + \sum_{i=2}^{\ell} \left[P_{k,j,i} \cdot \Pr \left(\|\mathbf{\Pi}^{(j)} \mathbf{h}_k\|^2 < c \left(\frac{\delta_i^{(j)}}{2^{R^{th}} - 1} - \sum_{m=1}^{i-1} \delta_m^{(j)} \right)^{-1} \cdot \frac{K}{\ell} \cdot P_t^{-1} \right) \right], \end{aligned} \quad (56)$$

where the threshold for $\|\mathbf{\Pi}^{(j)} \mathbf{h}_k\|^2$ in the second term in (56) is obtained by manipulation of the second term in (55). By Lemma 4 in Appendix D, there always exists a collection of in-group power distribution

factors $(\delta_1^{(j)}, \dots, \delta_\ell^{(j)})$ such that $(\frac{\delta_i^{(j)}}{2^{R^{th}}-1} - \sum_{m=1}^{i-1} \delta_m^{(j)})$ in (56) is strictly positive for all $i = 2, \dots, \ell$. Set $(\delta_1^{(j)}, \dots, \delta_\ell^{(j)})$ as one of such collections. Then, each probability term in (56) behaves as $P_t^{-N(K-k+1)}$ as $P_t \rightarrow \infty$, since $\|\mathbf{\Pi}^{(j)} \mathbf{h}_k\|^2$ has the same degrees of freedom of $N(K-k+1)$ in (38) and (39) as $\|\mathbf{h}_k\|^2$ by Proposition 2. Hence, their linear combination (54) behaves as $P_t^{-N(K-k+1)}$ as $P_t \rightarrow \infty$, and furthermore the term (49) as a linear combination of terms (54) behaves as $P_t^{-N(K-k+1)}$ as $P_t \rightarrow \infty$. Now, by adding (49) and the term in (42), we have the exact outage probability. We already showed that the term in (42) behaves as $P_t^{-N(K-k+1)}$ as $P_t \rightarrow \infty$. Furthermore, the upper bound of (49) behaves as $P_t^{-N(K-k+1)}$ as $P_t \rightarrow \infty$. Hence, we have $-D_k = \lim_{P_t \rightarrow \infty} \frac{\log \Pr(R_k < R^{th})}{\log P_t} \leq -N(K-k+1)$. Combining this upper bound result with the lower bound result, we have

$$N(K-k+1) \leq D_k = - \lim_{P_t \rightarrow \infty} \frac{\log \Pr(R_k < R^{th})}{\log P_t} \leq N(K-k+1). \quad (57)$$

■

Corollary 1: For the Gaussian MISO BC with N transmit antennas and K single-antenna users with independent Rayleigh fading described in Section II-A, the diversity order of the overall system achievable by the mixture transceiver architecture with the proposed user grouping method is given by

$$D = N \quad (58)$$

Proof: The decay rate of the overall outage probability is dominated by the worst decay rate. The worst diversity order in Theorem 1 occurs when $k = K$, and is given by N . ■

Note that the diversity order of the full ZF downlink beamforming is given by [14]

$$D = N - K + 1. \quad (59)$$

Hence, a significant improvement in the diversity order is attained by the mixture scheme. Note that the possible maximum diversity order for user k with channel $\mathbf{h}_k \sim \mathcal{CN}(0, 2\mathbf{I})$ is simply N . Hence, the mixture transceiver architecture achieves the full diversity order N in MISO BCs.

A. Diversity and Multiplexing Trade-off

With the cluster power factors $\{\delta_i > 0, i = 1, \dots, L\}$ fixed, as the total cluster power P increases according to (17) without bound, in each group only the rate of the first user scales as $\log \text{SNR}$ but the rates of all other users saturate to constants: $\bar{R}_i^{(j)} = \log_2 \left(1 + \frac{\delta_i^{(j)}}{\sum_{m=1}^{i-1} \delta_m^{(j)}} \right)$, $i = 2, \dots, L$, as seen in

(19).[†] Hence, the multiplexing gain for one user group with superposition and SIC is one regardless of the number of users in the group. (A similar observation of multiplexing gain one per superposition-and-SIC user group was made in [24].) Thus, the overall multiplexing gain of the mixture scheme with the adaptive user grouping is the same as the number of user groups N_g which is less than or equal to $K(\leq N)$. Note that in the case of $K = N$, the multiplexing gain of the ZF beamforming is N , whereas its diversity order is one. Thus, diversity-order and multiplexing-gain trade-off known in single-user MIMO [25] occurs even in MISO BCs [26]. In fact, it can be shown by replacing L with K in Proposition 1 and going through the proof of Theorem 1 with $N_g = 1$ that the full diversity order N can be achieved by a single superposition-and-SIC group containing all K users without considering channel alignment and orthogonality at all. However, this single-group full superposition-and-SIC approach is not good since it yields multiplexing gain one regardless of channel realization. This scheme can be considered as an antipodal scheme of the ZF beamforming in terms of diversity and multiplexing trade-off: The diversity order and multiplexing gain of the full superposition-and-SIC approach versus full ZF beamforming are $(N, 1)$ versus $(1, N)$ for MISO BCs with $K = N$. On the other hand, the proposed user grouping method is adaptive and depends on the channel realization. The number of groups is not predetermined in the proposed user grouping method. The number of user groups can be K if all user channels are semi-orthogonal. The number of user groups can be one if all user channels are aligned. Hence, the number N_g of constructed user groups, i.e., the multiplexing gain of the mixture scheme with the adaptive user grouping method, is adaptive to channel realization, while the full diversity order N is always achieved. So, we can view that the mixture scheme with such an adaptive user grouping method tries to opportunistically increase the multiplexing gain while achieving the full diversity order. Note that N_g is a random variable under the assumption that $\mathbf{h}_k, k = 1, \dots, K$ are random, and it depends on the angle threshold between the user groups used in the adaptive user grouping algorithm. We were not able to compute an analytic form for the expectation of N_g to evaluate the multiplexing gain loss as compared to the ZF beamforming, but a numerical assessment of the multiplexing gain loss as compared to the ZF beamforming is provided in Section V.

V. NUMERICAL RESULTS

In this section, we provide some numerical results to validate our theoretical analysis in the previous sections. We considered the MISO BC described in Section II-A. In each simulation scenario, we

[†]The target rates of User $2, \dots, L$ for group \mathcal{G}_j should be less than $\bar{R}_i^{(j)}$, but δ_i 's can be designed for a common target rate R_{th} based on (86). Please see Section V-C.

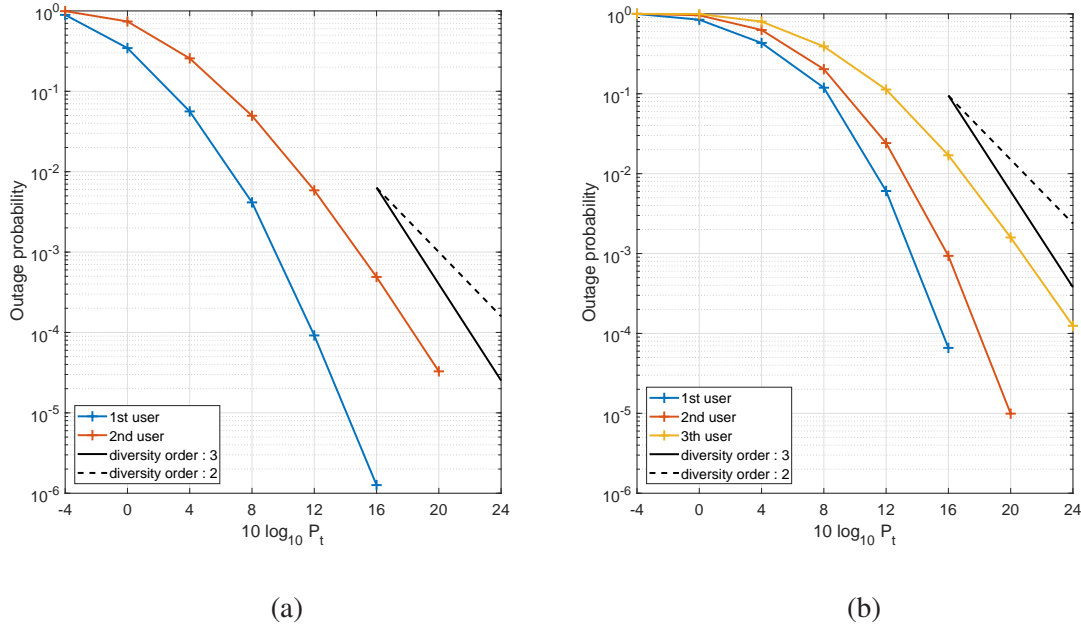


Fig. 3: Outage probability of the mixture transceiver architecture: (a) $N = 3, K = 2$ and (b) $N = 3, K = 3$

generated the K channel vectors $\mathbf{h}_1, \dots, \mathbf{h}_K$ of the system independently from the zero-mean complex Gaussian distribution $\mathcal{CN}(\mathbf{0}, 2\mathbf{I})$ sufficiently many times to numerically compute outage probability. For each channel realization, we ran the user grouping algorithm (Algorithm 1) with $\theta^{th} = 0.9$. With the constructed groups, we applied inter-group ZF beamforming and designed the intra-group beam vectors according to the constraint (17), i.e., $\mathbf{w}_1 = \dots = \mathbf{w}_L = \mathbf{w}^*$ with the solution \mathbf{w}^* to the max-min problem (70) used in the proof of Proposition 1. The rate R_k of the k -th user is obtained based on the designed beam vectors in this way. (Note that the beam vectors $\mathbf{w}_1 = \dots = \mathbf{w}_L = \mathbf{w}^*$ designed in this way yield rates larger than or equal to the lower bounds in (18) and (19).) For the intra-group beam design, the power distribution factors are chosen to satisfy the condition in Lemma 4 in Appendix D. The used values for power distribution factors are $(0.2, 0.8)$ for every two-user group, $(0.05, 0.2, 0.75)$ for every three-user group in Figs. 2(a), 2(b) and 3(a), and are the solution of (86) with $C = 2$ in Fig. 3(b). For computation of the outage probability $\Pr(R_k \leq R_{th})$, we set the target rate threshold as $R_{th} = 1.5$ [bits/channel use] in all simulations.

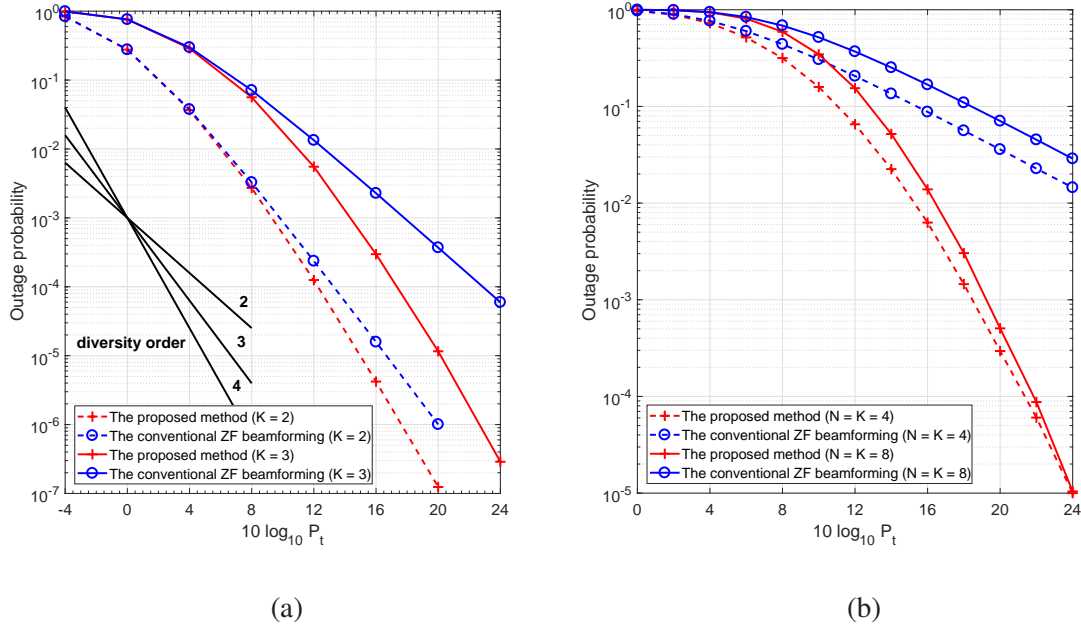


Fig. 4: Overall outage probability : (a) $N = 4$, $K = 2$ or 3 and (b) $N = K = 4$ and $N = K = 8$

A. Diversity Order Considering Order Statistic

First, we numerically evaluated the outage probability and diversity order of each user of the mixture transceiver architecture with considering channel norm ordering. Fig. 3 shows the outage probability of the mixture transceiver architecture in two cases: (a) $N = 3$, $K = 2$ and (b) $N = 3$ and $K = 3$, where User k is defined as the user with the k -th largest channel norm (i.e. $\|\mathbf{h}_1\|^2 \geq \|\mathbf{h}_2\|^2 \geq \dots \geq \|\mathbf{h}_K\|^2$). In the case (a) of $N = 3$, $K = 2$, Theorem 1 states that the diversity orders of Users 1 and 2 are 6 and 3, respectively. It is seen in Fig. 3(a) that the outage probability of User 2 has the slope corresponding to diversity order of 3, as SNR increases. It is also seen that the decay rate of User 1 is almost twice that of User 2. (In \log_{10} y-scale, roughly User 1 has -4 and -5.9 and User 2 has -2.2 and -3.3 at $10 \log P_t = 12$ and 16, respectively.) In the case (b) of $N = 3$, $K = 3$, Theorem 1 states that the diversity orders of Users 1, 2 and 3 are 9, 6, and 3, respectively. It is observed in Fig. 3(b) that the outage probability of User 3 has the slope corresponding to diversity order of 3, as SNR increases.

B. Overall Diversity Order

Then, we compared the mixture transceiver architecture with the full ZF downlink beamforming, based on the overall system diversity order. In order to see the overall diversity order, we computed overall outage probability. For this, we neglected channel norm ordering and computed the total number of

outages occurred at all K users over all Monte Carlo runs. Fig. 4 shows the overall outage probability for the same channel statistics and the same rate threshold for the mixture scheme and the ZF downlink beamforming. We considered four cases: *i)* $N = 4, K = 2$ and *ii)* $N = 4, K = 3$ shown in Fig. 4(a) and *iii)* $N = K = 4$ and *iv)* $N = K = 8$ shown in Fig. 4(b). For the considered cases *i)*, *ii)*, *iii)*, and *iv)*, the corresponding system diversity orders of the mixture scheme are 4, 4, 4 and 8 by Corollary 1, whereas the corresponding diversity orders of the ZF downlink beamforming are 3, 2, 1, and 1 by (59). It is seen in Fig. 4(a) that indeed the diversity orders of cases *i)* and *ii)* for the mixture scheme are the same as four. (The two red curves in Fig. 4(a) seem to have the same slope with some offset, as SNR increases.) On the other hand, it is seen that the diversity orders of the ZF downlink beamforming depends on K for the same N , as expected. The outage performance result for the cases with more transmit antennas $N = K = 4$ and $N = K = 8$ is shown in Fig. 4(b). It is seen that the full ZF beamforming yields the same slope for the two cases $N = K = 4$ and $N = K = 8$, as expected, since it yields the diversity order of one in both cases by (59). On the other hand, it is seen that the diversity orders in the two cases $N = K = 4$ and $N = K = 8$ are different for the mixture scheme, as predicted by Corollary 1. Indeed, it is seen that the decay rate of the outage probability in the case of $N = K = 8$ is larger than that of the case of $N = K = 4$, although the outage probability of the case $N = K = 8$ is higher than that of the case $N = K = 4$ at low SNR. Note that the outage performance gain by the mixture scheme over the ZF beamforming is drastic in the case of $N = K = 4$ and $N = N = 8$ for the meaningful range where the outage probability is below 10^{-2} .

C. Rate Distribution and Multiplexing Gain Loss

Next, we investigated the actual rate distribution and the multiplexing gain loss of the mixture scheme as compared to the ZF beamforming. For a numerical study, we again considered the case of $N = K = 4$ considered in Fig. 4(b). For the power distribution factors $\delta_1, \dots, \delta_4$, we used (86) with $R_{th} = 1.5$ and $C = 2$. (Other simulation setting is the same as that for Fig. 4(b).) We know that the common target rate should be smaller than $\bar{R}_i^{(j)} = \log_2 \left(1 + \frac{\delta_i^{(j)}}{\sum_{m=1}^{i-1} \delta_m^{(j)}} \right)$, $i = 2, \dots, |\mathcal{G}_j|$ since the rates of the users except the first user in group \mathcal{G}_j saturate to $\bar{R}_i^{(j)}$, $i = 2, \dots, |\mathcal{G}_j|$. However, the power distribution factors $\delta_1^{(j)}, \dots, \delta_{|\mathcal{G}_j|}^{(j)}$ of group \mathcal{G}_j can be designed for the target rate R_{th} by using (86). Note that channel realization does not satisfy the target rate R_{th} with 100 percents and it is just a target rate. Hence, outage can still occur for the designed target rate with small probability. (86) with $R_{th} = 1.5$ and $C = 2$ yields the following power distribution factor values:

- $\delta_1^{(j)} = 1$ for the first user in any group with cardinality one.

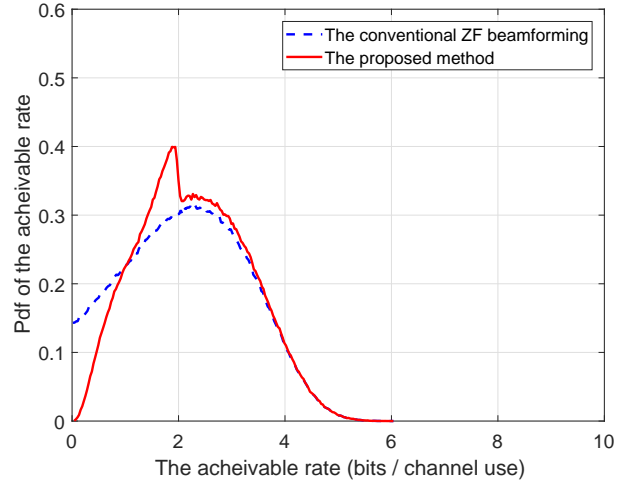
- $\delta_1^{(j)} = 0.2071$, $\delta_2^{(j)} = 0.7929$ for the first and second users in any group with cardinality two.
- $\delta_1^{(j)} = 0.0429$, $\delta_2^{(j)} = 0.1642$, $\delta_3^{(j)} = 0.7929$ for the first, second and third users in any group with cardinality three.
- $\delta_1^{(j)} = 0.0089$, $\delta_2^{(j)} = 0.0340$, $\delta_3^{(j)} = 0.1642$, $\delta_4^{(j)} = 0.7929$ for the first, second, third and fourth users in any group with cardinality four.

The corresponding $\bar{R}_i^{(j)}$ is given as follows:

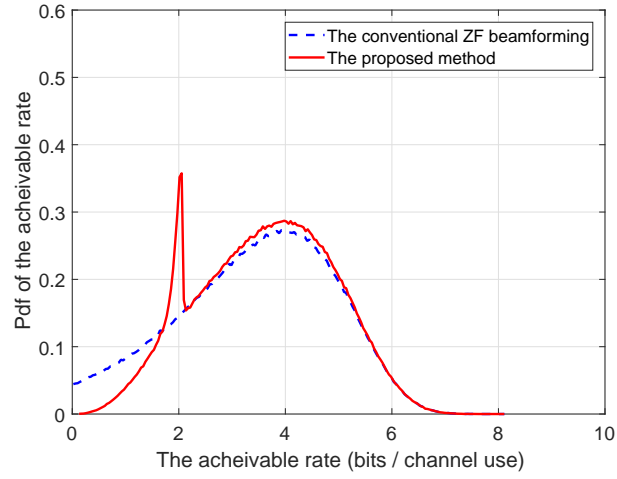
- $\bar{R}_2^{(j)} = 2.2716$ for the second user in any group with cardinality two.
- $\bar{R}_2^{(j)} = 2.2713$, $\bar{R}_3^{(j)} = 2.2716$ for the second and third users in any group with cardinality three.
- $\bar{R}_2^{(j)} = 2.2691$, $\bar{R}_3^{(j)} = 2.2713$, $\bar{R}_3^{(j)} = 2.2716$ for the second, third and fourth users in any group with cardinality four.

Note that (86) with $R_{th} = 1.5$ and $C = 2$ yields the power distribution factor values so that the rate upper bound $\bar{R}_i^{(j)}$ for non-first users is set just above the target rate R_{th} . The margin is controlled by the constant C . Hence, when a common target rate is given, we can design the power distribution factors $\delta_i^{(j)}$ such that the rate upper bound $\bar{R}_i^{(j)}$ for non-first users is set just above the target rate R_{th} by using (86).

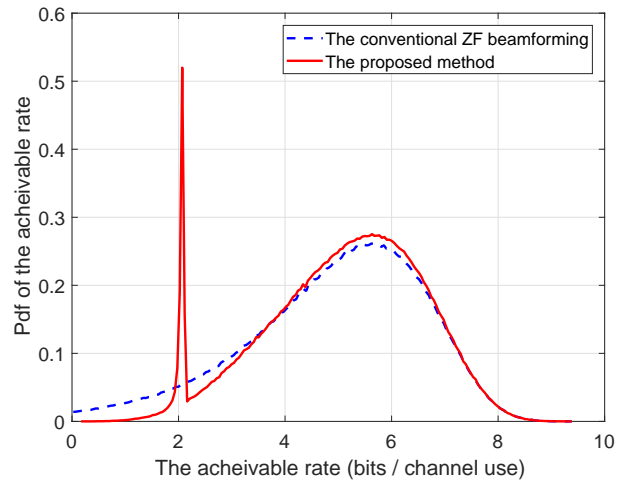
For the $N = K = 4$ system, we considered $10 \log_{10} \frac{P}{1} = [10, 15, 20, 40, 60]$ dB, where one in the denominator is the noise variance. For each SNR point, we generated 500,000 channel realizations. For each channel realization, we applied the ZF beamforming and the mixture scheme and obtained the rates of the four users in the system. With the overall $4 \times 500,000$ rate values, we obtained the rate distribution with the histogram method. The rate distribution results are shown in Figs. 5 and 6. Note that the mixture scheme with adaptive user grouping is opportunistic in multiplexing gain and at least multiplexing gain of one is guaranteed since the number of groups is equal to or larger than one. It is observed that the rate distribution of the mixture scheme is a mixture of the first users' rate distribution and the non-first users' rate distribution. The distribution component of the first users' rates shows a similar distribution to that of the ZF scheme. That is, as SNR increases, the first users' rate distribution shifts to the right in the figures. We also see the component of the distribution of the non-first users's rates. This component accumulates around $R \approx 2.2$ as predicted by the above values of $\bar{R}_i^{(j)}$. As SNR increases, the accumulation becomes sharper looking like a peak just below $\bar{R}_i^{(j)}$. Note the rate lower tail behaviors of the mixture scheme and the ZF scheme. At SNR = 10, 15, 20 dB, the mixture has much lighter tails. At SNR=20 dB, the mixture scheme yields most rates above the target rate $R_{th} = 1.5$, whereas still quite a portion is below the target rate $R_{th} = 1.5$ with the ZF scheme. Even at SNR=40dB, we can still see the non-zero tail



(a)



(b)



(c)

Fig. 5: Rate distribution ($N = K = 4$) (a) $10 \log \frac{P_t}{1} = 10\text{dB}$, (b) $10 \log \frac{P_t}{1} = 15\text{dB}$, (c) $10 \log \frac{P_t}{1} = 20\text{dB}$

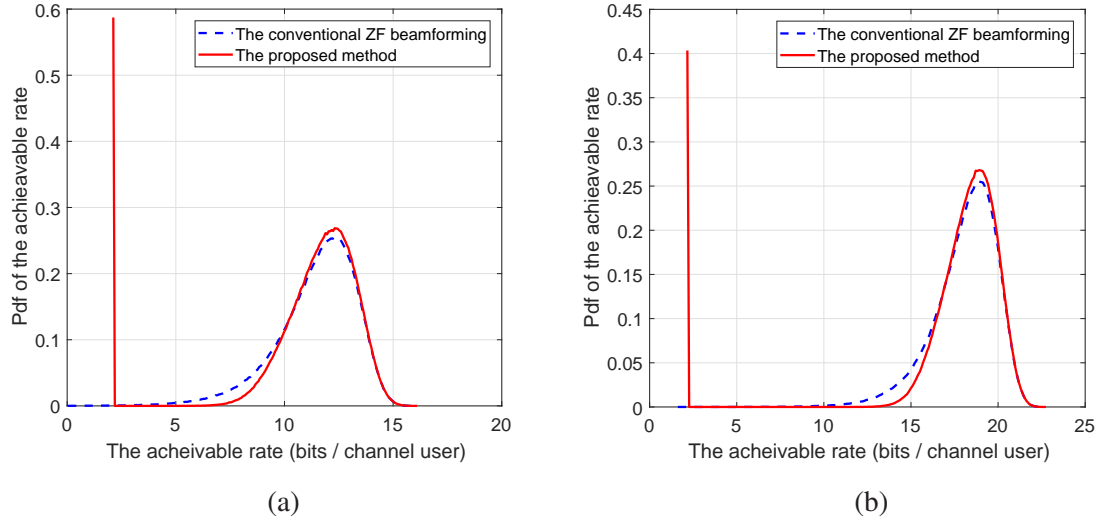


Fig. 6: Rate distribution ($N = K = 4$) (a) $10 \log \frac{P_t}{1} = 40\text{dB}$ and (b) $10 \log \frac{P_t}{1} = 60\text{dB}$

around the origin for the ZF scheme, whereas for the mixture scheme the rate distribution starts from R_{th} with a sharp peak. Note that the first users' rates of the mixture scheme almost match those of the ZF scheme. However, still there is a large peak around $\bar{R}_i^{(j)}$ due to the non-first users for the mixture scheme, and this reduces the multiplexing gain of the mixture scheme.

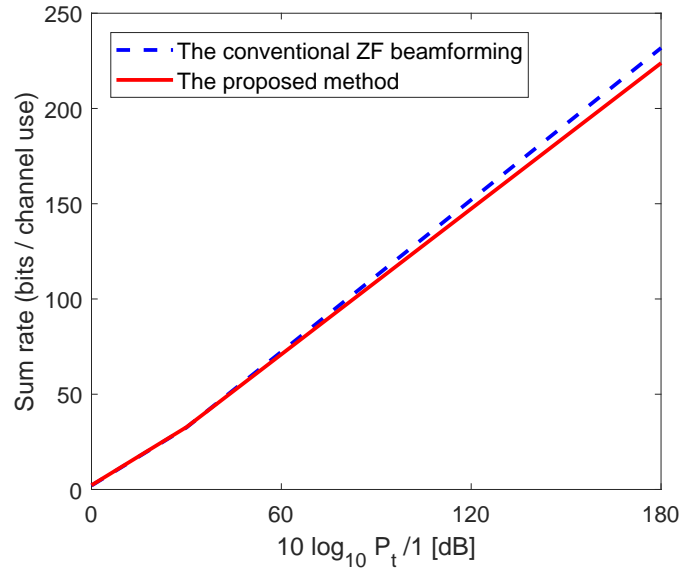


Fig. 7: Average sum rate: $K = N = 4$

Hence, we further investigated the multiplexing gain, i.e., the slope of rate increase with respect to SNR. For each SNR point, we averaged the rates of the four users in the system over channel realizations. Then, we plotted the average rates of the mixture scheme and the ZF scheme with respect to SNR. The result is shown in Fig. 7. It is seen that the multiplexing gain loss of the mixture scheme compared to the ZF scheme is insignificant at least in the case of $N = K = 4$.

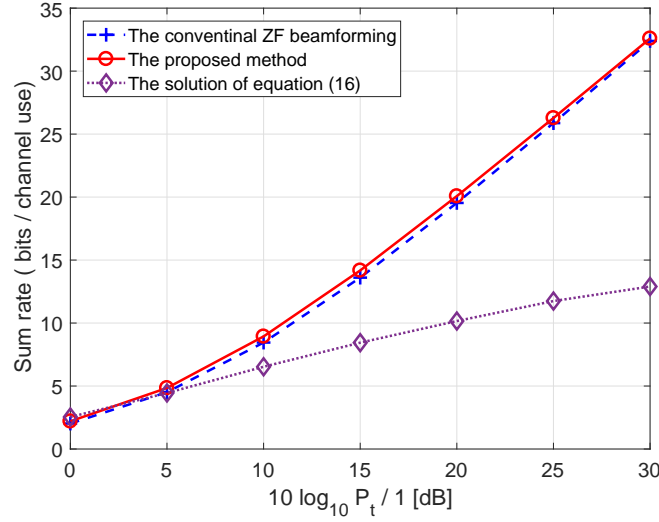


Fig. 8: Average sum rate: $K = N = 4$

We further investigated the performance of the single-group approach with more sophisticated beam design obtained by solving the problem (16). We solved the problem (16) for the $N = K = 4$ system considered above as a single group with superposition and SIC. Since the problem (16) is non-convex, several steps are needed. First, we transform the problem (16) into a problem of maximizing sum rate with feasible power ratio-tuples. Then, it is reformulated as maximizing the geometric mean of SINRs with non-convex constraints [18]. Next, we approximate the non-convex constraints using the convex concave procedure [19] and can solve the problem in an iterative manner. Sweeping $(p_1, p_2, \dots, p_K) = (\delta_1 P_t, \delta_2 P_t, \dots, \delta_K P_t)$ yields a rate region. However, we did not perform this sweeping since our goal is not to obtain a rate region. Instead, we determined $(p_1, p_2, \dots, p_K) = (\delta_1 P_t, \delta_2 P_t, \dots, \delta_K P_t)$ based on (86) with $C = 2$ and $R_{th} = 1.5$ and computed the corresponding sum rate of the problem (16). The corresponding rate-tuple point is on the boundary of the rate region of (16), although it may not be the sum-rate maximizing point. The result is shown in Fig. 8. The curves of the proposed method and the conventional ZF method are the same as those in Fig. 7, and the curve of the solution of the problem (16)

with $(p_1, p_2, \dots, p_K) = (\delta_1 P_t, \delta_2 P_t, \dots, \delta_K P_t)$ determined based on (86) with $C = 2$ and $R_{th} = 1.5$ is newly added. Even though we solve the problem (16) optimally based on the aforementioned complicated procedure not based on user grouping, inter-group ZF, in-group simple superposition beamforming $\mathbf{w}_1 = \dots = \mathbf{w}_K$, the resulting rate of the problem (16) with a single-group approach is not good. Note that the corresponding slope is much smaller than that of the ZF scheme and the proposed scheme. This is because as mentioned before, if we group all users in a single group and apply superposition and SIC, we have the multiplexing gain of only one, whatever sophisticated beam design and power allocation are used. Even if we adjust power allocation to yield maximum sum rate, this does not change the slope, i.e., the multiplexing gain. On the other hand, the full ZF beamforming has the multiplexing gain of four and the mixture scheme with adaptive user grouping has the multiplexing gain from one to four. On average, the multiplexing gain of the mixture scheme with adaptive user grouping slightly falls short of four, as seen in Fig. 7. So, it is more important to group users properly to yield as many groups as possible, while maintaining minimum inter-group angle separation, rather than to apply a sophisticated beam design method with one overall group from the perspective of the multiplexing gain, i.e., the sum rate.

Now how to operate the mixture scheme is clear. Consider MISO-BC URLLC in which no retransmission is allowed due to latency constraint (one round-trip delay for retransmission is in the order of 10 ms, whereas URLLC requires 1ms delay) and low-latency low-data-rate packets should be delivered reliably. First, we determine the angle threshold between group channel subspaces to be not too large so that we have as many groups as possible but we still avoid angle-wise very close groups. We determine the minimum target rate that should be satisfied by all users for URLLC. With the target rate, we design the power distribution factors, and run the adaptive user grouping. For the first users in the constructed groups, we can still apply rate adaptation based on modulation level and coding rate by exploiting the supportable rate channel quality indicator (CQI). (The distribution of the first users' rates is wide across the x-axis in Fig. 5 and 6. We should exploit this.) But, for the non-first users we just transmit data with the target rate. In fact, we can control the first user in each group. In the case that a user wanted as the first user does not have maximum effective channel norm, we assign more power to the wanted user so that more power times its effective channel gain surpasses the largest effective channel norm of other user in the group. Then, we distribute the remaining group power according to (86) with the target rate R_{th} . With this, we can control the mixture system so that any user can be a high-rate first user while supporting the target rate with high reliability.

D. Comparison with Other Advanced Transceiver Designs for MISO BCs

We considered other advanced transceiver designs for MISO BCs, e.g., [27], [28], devised to improve the performance over ZF downlink beamforming, and compared the outage performance of these advanced designs with the mixture architecture. The result is shown in Fig. 9, where the setup is $N = K = 4$ and other parameter setting is the same as that in Fig. 4(b) with $N = K = 4$. It is seen that the advanced transceiver designs having the full multiplexing gain yield the same diversity order as the ZF beamforming, which is worse than that of our scheme, although they yield better rates compared to the ZF beamforming. Thus, these advanced designs are at the multiplexing-gain-optimal side in terms of diversity-and-multiplexing trade-off.

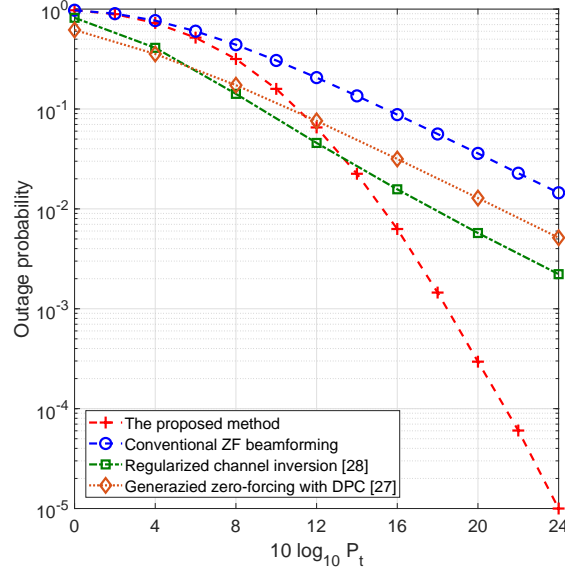
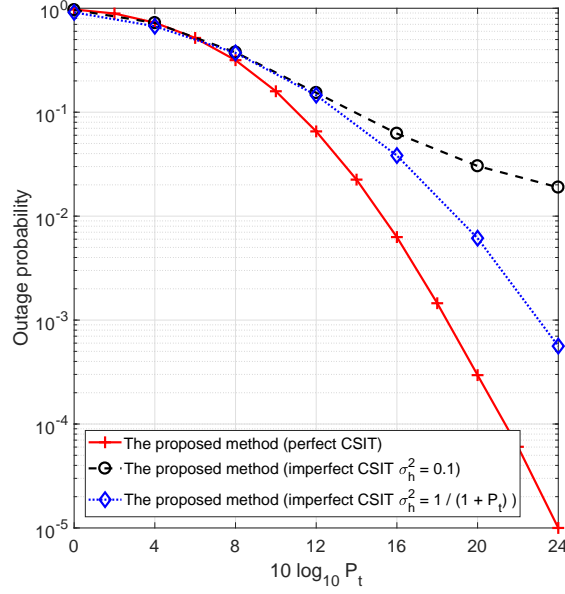


Fig. 9: Comparison with other advanced methods: $K = N = 4$

E. Impact of Imperfect CSI

Although analysis of the outage performance under imperfect CSIT is beyond the scope of this paper, we briefly investigated the impact of imperfect CSIT through simulation. Again we considered the case of $N = K = 4$ with the same other setting as that in Fig. 4(b). It is known that the number of CSI feedback bits per user should increase linearly with respect to SNR (or signal power for fixed noise variance) in log scale in order to achieve full multiplexing gain for MISO BCs [29]. For simulation the CSI error is assumed to be zero-mean Gaussian with variance σ_e^2 , where we set 1) σ_e^2 as a fixed constant of 0.1 and

Fig. 10: Impact of imperfect CSI: $K = N = 4$

2) $\sigma_e^2 = \frac{1}{1+P_t}$ to be consistent with the result in [29]. The result is shown in Fig. 10. It is seen that the fixed CSI quality with respect to SNR shows a floor for the outage probability as SNR increases. On the other hand, the CSI with quality $\sigma_e^2 = \frac{1}{1+P_t}$ does not show such a floor behavior. Indeed, it seems that the increasing CSI quality with respect to SNR is required to achieve the full diversity order although the exact increasing rate is not known yet.

VI. CONCLUSION

In this paper, we have considered the mixture transceiver architecture with channel-adaptive user grouping and mixture of linear and nonlinear SIC reception for MISO BCs, and have shown that the mixture transceiver architecture opportunistically increases the multiplexing gain while achieving full diversity order for MISO BCs. The mixture transceiver architecture can provide far better outage performance compared to the widely-used conventional ZF downlink beamforming for MU-MISO BCs under channel fading environments. The gain in diversity order results from possible sacrifice of multiplexing gain through diversity-and-multiplexing trade-off, and thus the mixture scheme provides an alternative transceiver architecture for MISO BCs to applications such as emerging URLLC in which reliability is more important than data rate. Future research directions include optimization of angle threshold and power distribution, finding optimal diversity-and-multiplexing trade-off in MISO BCs, finding faster

grouping algorithms scalable with the number of users for large systems, application of the mixture architecture to the uplink [15], and application of more advanced transmit signaling [30].

APPENDIX A: PROOF OF PROPOSITION 1

For given $(\delta_1, \dots, \delta_L)$, in order to obtain a lower bound on the achievable rate of each user, we simply set $\mathbf{w}_1 = \mathbf{w}_2 = \dots = \mathbf{w}_L = \mathbf{w}$ with $\|\mathbf{w}\|^2 \leq 1$ as in the constraint (17), i.e., we consider that all L users use the same beam vector. Then, the rates in (14) of the MISO BC with superposition coding and SIC can be rewritten as

$$R_1 = \log_2 (1 + \delta_1 P |\mathbf{g}_1^H \mathbf{w}|^2) \quad (60)$$

$$\begin{aligned} R_i &= \log_2 \left(1 + \min \left\{ \frac{\delta_i P |\mathbf{g}_1^H \mathbf{w}|^2}{\sum_{m=1}^{i-1} \delta_m P |\mathbf{g}_1^H \mathbf{w}|^2 + 1}, \dots, \frac{\delta_i P |\mathbf{g}_i^H \mathbf{w}|^2}{\sum_{m=1}^{i-1} \delta_m P |\mathbf{g}_i^H \mathbf{w}|^2 + 1} \right\} \right), \quad i = 2, \dots, L, \\ &= \log_2 \left(1 + \frac{\delta_i}{\sum_{m=1}^{i-1} \delta_m} \cdot \frac{1}{1 + 1/\left[\min\{|\mathbf{g}_1^H \mathbf{w}|^2, \dots, |\mathbf{g}_i^H \mathbf{w}|^2\}(\sum_{m=1}^{i-1} \delta_m)P\right]} \right). \end{aligned} \quad (61)$$

Using Lemma 2 below, we can bound the terms $|\mathbf{g}_1^H \mathbf{w}|^2$ in (60) and $\min\{|\mathbf{g}_1^H \mathbf{w}|^2, \dots, |\mathbf{g}_i^H \mathbf{w}|^2\}$ in (61) as follows: Using the optimal solution \mathbf{w}^* to the max-min problem (70), we have

$$|\mathbf{g}_1^H \mathbf{w}^*|^2 \geq \min \left\{ \left| \left(\frac{\mathbf{g}_1}{\|\mathbf{g}_1\|} \right)^H \mathbf{w}^* \right|^2, \dots, \left| \left(\frac{\mathbf{g}_L}{\|\mathbf{g}_L\|} \right)^H \mathbf{w}^* \right|^2 \right\} \|\mathbf{g}_1\|^2 \quad (62)$$

$$\geq \frac{1}{c} \|\mathbf{g}_1\|^2, \quad (63)$$

where (62) is valid since the minimum is taken over multiple terms including $|\mathbf{g}_1^H \mathbf{w}^*|^2$, and (63) is valid by Lemma 2 below. Next, we have

$$\min\{|\mathbf{g}_1^H \mathbf{w}^*|^2, \dots, |\mathbf{g}_i^H \mathbf{w}^*|^2\} = \min \left\{ \left| \left(\frac{\mathbf{g}_1}{\|\mathbf{g}_i\|} \right)^H \mathbf{w}^* \right|^2, \dots, \left| \left(\frac{\mathbf{g}_i}{\|\mathbf{g}_i\|} \right)^H \mathbf{w}^* \right|^2 \right\} \|\mathbf{g}_i\|^2 \quad (64)$$

$$\geq \min \left\{ \left| \left(\frac{\mathbf{g}_1}{\|\mathbf{g}_1\|} \right)^H \mathbf{w}^* \right|^2, \dots, \left| \left(\frac{\mathbf{g}_i}{\|\mathbf{g}_i\|} \right)^H \mathbf{w}^* \right|^2 \right\} \|\mathbf{g}_i\|^2 \quad (65)$$

$$\geq \min \left\{ \left| \left(\frac{\mathbf{g}_1}{\|\mathbf{g}_1\|} \right)^H \mathbf{w}^* \right|^2, \dots, \left| \left(\frac{\mathbf{g}_L}{\|\mathbf{g}_L\|} \right)^H \mathbf{w}^* \right|^2 \right\} \|\mathbf{g}_i\|^2 \quad (66)$$

$$\geq \frac{1}{c} \|\mathbf{g}_i\|^2, \quad (67)$$

where (65) is valid since $\|\mathbf{g}_1\| \geq \dots \geq \|\mathbf{g}_L\|$, (66) is valid since we increased the number of terms in the minimization including the previous terms, and (67) holds by Lemma 2 below. Substituting (63) and (67) into (60) and (61), respectively, we have the rates that can be achieved by the optimal solution $\mathbf{w}^* = \mathbf{w}_1 = \dots = \mathbf{w}_L$ to the max-min problem (70):

$$R_1 \geq \log_2 \left(1 + \frac{1}{c} \delta_1 \|\mathbf{g}_1\|^2 P \right) \quad (68)$$

$$R_i \geq \log_2 \left(1 + \frac{\delta_i}{\sum_{m=1}^{i-1} \delta_m} \frac{1}{1 + \left(\frac{1}{c} \|\mathbf{g}_i\|^2 \sum_{m=1}^{i-1} \delta_m P \right)^{-1}} \right), \quad i = 2, \dots, L. \quad (69)$$

The considered design here of $\mathbf{w}_1 = \dots = \mathbf{w}_L = \mathbf{w}^*$ with $\|\mathbf{w}^*\|^2 \leq 1$ and $p_i = \delta_i P$ with $(\delta_1, \dots, \delta_L) \in \mathcal{D}$, i.e., (17), satisfies the original beam design constraint $(\mathbf{w}_1, \dots, \mathbf{w}_L) \in \mathcal{W}^L$ and $p_i > 0, \forall i, \sum_{i=1}^L p_i = P$ in (16). Hence, the rates achieved by $\mathbf{w}_1 = \dots = \mathbf{w}_L = \mathbf{w}^*$ with $(\delta_1, \dots, \delta_L)$ are lower bounds on the achievable rates. \blacksquare

Lemma 2: Consider the following max-min optimization problem:

$$\begin{aligned} \max \quad & \min \left\{ \left| \left(\frac{\mathbf{g}_1}{\|\mathbf{g}_1\|} \right)^H \mathbf{w} \right|^2, \dots, \left| \left(\frac{\mathbf{g}_L}{\|\mathbf{g}_L\|} \right)^H \mathbf{w} \right|^2 \right\} \\ \text{subject to} \quad & \|\mathbf{w}\|^2 \leq 1. \end{aligned} \quad (70)$$

The optimal solution \mathbf{w}^* to the problem (70) satisfies the following:

$$\min \left\{ \left| \left(\frac{\mathbf{g}_1}{\|\mathbf{g}_1\|} \right)^H \mathbf{w}^* \right|^2, \dots, \left| \left(\frac{\mathbf{g}_L}{\|\mathbf{g}_L\|} \right)^H \mathbf{w}^* \right|^2 \right\} \geq \frac{1}{c}, \quad (71)$$

where

$$c = \begin{cases} L & \text{if } L \leq 3, \\ 8L^2 & \text{if } L > 3. \end{cases} \quad (72)$$

Proof of Lemma 2: Define unit-norm $\mathbf{v}_i := \mathbf{g}_i / \|\mathbf{g}_i\|$ for $i = 1, \dots, L$. Then, (70) can be rewritten as

$$\begin{aligned} \max \quad & \min \left\{ |\mathbf{v}_1^H \mathbf{w}|^2, \dots, |\mathbf{v}_L^H \mathbf{w}|^2 \right\} \\ \text{subject to} \quad & \|\mathbf{w}\|^2 \leq 1 \end{aligned} \quad (73)$$

The problem (73) can be reformulated as

$$\max \frac{\min \left\{ |\mathbf{v}_1^H \mathbf{w}|^2, \dots, |\mathbf{v}_L^H \mathbf{w}|^2 \right\}}{\|\mathbf{w}\|^2} = \min \frac{\|\mathbf{w}\|^2}{\min \left\{ |\mathbf{v}_1^H \mathbf{w}|^2, \dots, |\mathbf{v}_L^H \mathbf{w}|^2 \right\}}, \quad (74)$$

where inversion of the cost function is taken in the right-hand side (RHS) of (74). Thus, it is known that

the optimal value of the problem (73) is equivalent to the inverse of the optimal value of the following quadratic programming (QP) [31]:

$$\begin{aligned} \min \quad & \|\mathbf{w}\|^2 \\ \text{subject to} \quad & |\mathbf{v}_i^H \mathbf{w}|^2 \geq 1, \quad i = 1, \dots, L. \end{aligned} \quad (75)$$

The QP (75) can be solved by semi-definite relaxation of the rewritten form of (75) [31]:

$$\begin{aligned} \min \quad & \text{Tr}(\mathbf{W}) \\ \text{subject to} \quad & \text{Tr}(\mathbf{V}_i \mathbf{W}) \geq 1, \quad i = 1, \dots, L \end{aligned} \quad (76)$$

where $\mathbf{W} := \mathbf{w}\mathbf{w}^H$ and $\mathbf{V}_i := \mathbf{v}_i \mathbf{v}_i^H$, $i = 1, \dots, L$. Denote the optimal values of the optimization problems (75) and (76) by v_{qp}^* and v_{sdp}^* , respectively. Then, the relationship between v_{qp}^* and v_{sdp}^* is known as [32]

$$\begin{aligned} v_{qp}^* &= v_{sdp}^*, & \text{if } L \leq 3, \\ v_{qp}^* &\leq 8L \cdot v_{sdp}^*, & \text{if } L > 3. \end{aligned} \quad (77)$$

Furthermore, note that $\mathbf{W}' := \sum_{i=1}^L \mathbf{V}_i$ is feasible for the problem (76) since $\text{Tr}(\mathbf{V}_i \mathbf{W}') = \text{Tr}(\mathbf{V}_i \sum_{i=1}^L \mathbf{V}_i) \geq \sum_{i=1}^L \text{Tr}(\mathbf{V}_i \mathbf{V}_i) \geq \text{Tr}(\mathbf{V}_i \mathbf{V}_i) = 1$, and $\text{Tr}(\mathbf{W}') = L$. Hence, we have

$$v_{sdp}^* \leq L. \quad (78)$$

Hence, with the optimal solution \mathbf{w}^* to (73), we have

$$\min \left\{ |\mathbf{v}_1^H \mathbf{w}^*|^2, \dots, |\mathbf{v}_L^H \mathbf{w}^*|^2 \right\} \stackrel{(a)}{=} 1/v_{qp}^* \stackrel{(b)}{\geq} L/c \cdot 1/v_{sdp}^* \stackrel{(c)}{\geq} 1/c, \quad (79)$$

where c is given by (72). Here, Step (a) is valid due to the relationship between the original problem (73) and the QP (75); Step (b) is valid due to (77); and Step (c) is valid due to (78). \blacksquare

APPENDIX B: PROOF OF LEMMA 1

The block matrix inversion formula is given as follows:

$$\begin{bmatrix} \mathbf{C} & \mathbf{U} \\ \mathbf{V} & \mathbf{D} \end{bmatrix} = \begin{bmatrix} \mathbf{C}^{-1} + \mathbf{C}^{-1} \mathbf{U} (\mathbf{D} - \mathbf{V} \mathbf{C}^{-1} \mathbf{U})^{-1} \mathbf{V} \mathbf{C}^{-1} & -\mathbf{C}^{-1} \mathbf{U} (\mathbf{D} - \mathbf{V} \mathbf{C}^{-1} \mathbf{U})^{-1} \\ -(\mathbf{D} - \mathbf{V} \mathbf{C}^{-1} \mathbf{U})^{-1} \mathbf{V} \mathbf{C}^{-1} & (\mathbf{D} - \mathbf{V} \mathbf{C}^{-1} \mathbf{U})^{-1} \end{bmatrix}, \quad (80)$$

which is used in Step (a) in the below.

$$\begin{aligned}
\Pi_{[\mathbf{A}, \mathbf{B}]}^\perp &= \mathbf{I} - [\mathbf{A} \ \mathbf{B}] \begin{bmatrix} \mathbf{A}^H \mathbf{A} & \mathbf{A}^H \mathbf{B} \\ \mathbf{B}^H \mathbf{A} & \mathbf{B}^H \mathbf{B} \end{bmatrix}^{-1} \begin{bmatrix} \mathbf{A}^H \\ \mathbf{B}^H \end{bmatrix} \\
&\stackrel{(a)}{=} \mathbf{I} - [\mathbf{A} \ \mathbf{B}] \begin{bmatrix} (\mathbf{A}^H \mathbf{A})^{-1} + (\mathbf{A}^H \mathbf{A})^{-1} \mathbf{A}^H \mathbf{B} (\mathbf{B}^H \mathbf{B} - \mathbf{B}^H \mathbf{A} (\mathbf{A}^H \mathbf{A})^{-1} \mathbf{A}^H \mathbf{B})^{-1} \mathbf{B}^H \mathbf{A} (\mathbf{A}^H \mathbf{A})^{-1}, \\ -(\mathbf{B}^H \mathbf{B} - \mathbf{B}^H \mathbf{A} (\mathbf{A}^H \mathbf{A})^{-1} \mathbf{A}^H \mathbf{B})^{-1} \mathbf{B}^H \mathbf{A} (\mathbf{A}^H \mathbf{A})^{-1}, \\ -(\mathbf{A}^H \mathbf{A})^{-1} \mathbf{A}^H \mathbf{B} (\mathbf{B}^H \mathbf{B} - \mathbf{B}^H \mathbf{A} (\mathbf{A}^H \mathbf{A})^{-1} \mathbf{A}^H \mathbf{B})^{-1} \\ (\mathbf{B}^H \mathbf{B} - \mathbf{B}^H \mathbf{A} (\mathbf{A}^H \mathbf{A})^{-1} \mathbf{A}^H \mathbf{B})^{-1} \end{bmatrix} \begin{bmatrix} \mathbf{A}^H \\ \mathbf{B}^H \end{bmatrix} \\
&= \mathbf{I} - \mathbf{A} (\mathbf{A}^H \mathbf{A})^{-1} \mathbf{A}^H - \mathbf{A} (\mathbf{A}^H \mathbf{A})^{-1} \mathbf{A}^H \mathbf{B} (\mathbf{B}^H \mathbf{B} - \mathbf{B}^H \mathbf{A} (\mathbf{A}^H \mathbf{A})^{-1} \mathbf{A}^H \mathbf{B})^{-1} \mathbf{B}^H \mathbf{A} (\mathbf{A}^H \mathbf{A})^{-1} \mathbf{A}^H \\
&\quad + \mathbf{B} (\mathbf{B}^H \mathbf{B} - \mathbf{B}^H \mathbf{A} (\mathbf{A}^H \mathbf{A})^{-1} \mathbf{A}^H \mathbf{B})^{-1} \mathbf{B}^H \mathbf{A} (\mathbf{A}^H \mathbf{A})^{-1} \mathbf{A}^H \\
&\quad + \mathbf{A} (\mathbf{A}^H \mathbf{A})^{-1} \mathbf{A}^H \mathbf{B} (\mathbf{B}^H \mathbf{B} - \mathbf{B}^H \mathbf{A} (\mathbf{A}^H \mathbf{A})^{-1} \mathbf{A}^H \mathbf{B})^{-1} \mathbf{B}^H \\
&\quad - \mathbf{B} (\mathbf{B}^H \mathbf{B} - \mathbf{B}^H \mathbf{A} (\mathbf{A}^H \mathbf{A})^{-1} \mathbf{A}^H \mathbf{B})^{-1} \mathbf{B}^H \\
&= \mathbf{I} - \Pi_{\mathbf{A}} - \Pi_{\mathbf{A}} \mathbf{B} (\mathbf{B}^H \Pi_{\mathbf{A}}^\perp \mathbf{B})^{-1} (\Pi_{\mathbf{A}} \mathbf{B})^H + \mathbf{B} (\mathbf{B}^H \Pi_{\mathbf{A}}^\perp \mathbf{B})^{-1} (\Pi_{\mathbf{A}} \mathbf{B})^H \\
&\quad + \Pi_{\mathbf{A}} \mathbf{B} (\mathbf{B}^H \Pi_{\mathbf{A}}^\perp \mathbf{B})^{-1} \mathbf{B}^H - \mathbf{B} (\mathbf{B}^H \Pi_{\mathbf{A}}^\perp \mathbf{B})^{-1} \mathbf{B}^H \\
&= \mathbf{I} - \Pi_{\mathbf{A}} - (\mathbf{B} - \Pi_{\mathbf{A}} \mathbf{B}) (\mathbf{B}^H \Pi_{\mathbf{A}}^\perp \mathbf{B})^{-1} (\mathbf{B} - \Pi_{\mathbf{A}} \mathbf{B})^H \\
&= \Pi_{\mathbf{A}}^\perp - \Pi_{\mathbf{A}}^\perp \mathbf{B} (\mathbf{B}^H \Pi_{\mathbf{A}}^\perp \mathbf{B})^{-1} (\Pi_{\mathbf{A}}^\perp \mathbf{B})^H \\
&= \Pi_{\mathbf{A}}^\perp - \Pi_{\mathbf{A}}^\perp \mathbf{B} ((\Pi_{\mathbf{A}}^\perp \mathbf{B})^H \Pi_{\mathbf{A}}^\perp \mathbf{B})^{-1} (\Pi_{\mathbf{A}}^\perp \mathbf{B})^H
\end{aligned}$$

where $\Pi_{\mathbf{A}} = \mathbf{A} (\mathbf{A}^H \mathbf{A})^{-1} \mathbf{A}^H$, $\Pi_{\mathbf{A}}^\perp = \mathbf{I} - \mathbf{A} (\mathbf{A}^H \mathbf{A})^{-1} \mathbf{A}^H$, and the block matrix inversion formula is used in Step (a). In the last equality, we used $\Pi_{\mathbf{A}}^{\perp H} \Pi_{\mathbf{A}}^\perp = (\Pi_{\mathbf{A}}^\perp)^2 = \Pi_{\mathbf{A}}^\perp$. Therefore, we have

$$\begin{aligned}
\Pi_{[\mathbf{A}, \mathbf{B}]}^\perp \mathbf{x} &= \Pi_{\mathbf{A}}^\perp \mathbf{x} - \Pi_{\mathbf{A}}^\perp \mathbf{B} ((\Pi_{\mathbf{A}}^\perp \mathbf{B})^H \Pi_{\mathbf{A}}^\perp \mathbf{B})^{-1} (\Pi_{\mathbf{A}}^\perp \mathbf{B})^H \mathbf{x} \\
&= \Pi_{\mathbf{A}}^\perp \mathbf{x} - \Pi_{\mathbf{A}}^\perp \mathbf{B} ((\Pi_{\mathbf{A}}^\perp \mathbf{B})^H \Pi_{\mathbf{A}}^\perp \mathbf{B})^{-1} (\Pi_{\mathbf{A}}^\perp \mathbf{B})^H (\Pi_{\mathbf{A}} \mathbf{x} + \Pi_{\mathbf{A}}^\perp \mathbf{x}) \\
&\stackrel{(b)}{=} \Pi_{\mathbf{A}}^\perp \mathbf{x} - \Pi_{\mathbf{A}}^\perp \mathbf{B} ((\Pi_{\mathbf{A}}^\perp \mathbf{B})^H \Pi_{\mathbf{A}}^\perp \mathbf{B})^{-1} (\Pi_{\mathbf{A}}^\perp \mathbf{B})^H \Pi_{\mathbf{A}}^\perp \mathbf{x} \\
&= (\mathbf{I} - \Pi_{\mathbf{A}}^\perp \mathbf{B} ((\Pi_{\mathbf{A}}^\perp \mathbf{B})^H \Pi_{\mathbf{A}}^\perp \mathbf{B})^{-1} (\Pi_{\mathbf{A}}^\perp \mathbf{B})^H) \Pi_{\mathbf{A}}^\perp \mathbf{x} \\
&= (\mathbf{I} - \Pi_{\Pi_{\mathbf{A}}^\perp \mathbf{B}}) \Pi_{\mathbf{A}}^\perp \mathbf{x},
\end{aligned}$$

where Step (b) holds because $\Pi_{\mathbf{A}}^\perp \mathbf{B} ((\Pi_{\mathbf{A}}^\perp \mathbf{B})^H \Pi_{\mathbf{A}}^\perp \mathbf{B})^{-1} (\Pi_{\mathbf{A}}^\perp \mathbf{B})^H$ is the projection onto $\mathcal{C}(\Pi_{\mathbf{A}}^\perp \mathbf{B})$ which is a subspace contained in $\mathcal{C}^\perp(\mathbf{A})$. ■

APPENDIX C: PROOF OF PROPOSITION 2

Consider the effective channel $\mathbf{g}_i^{(j)} = \Pi_{\tilde{\mathbf{H}}_j}^\perp \mathbf{h}_i^{(j)}$, where $\mathbf{h}_i^{(j)}$ is the channel vector of User i in group \mathcal{G}_j , and $\tilde{\mathbf{H}}_j$ is defined in (10). By Lemma 1, $\mathbf{g}_i^{(j)} = \Pi_{\tilde{\mathbf{H}}_j}^\perp \mathbf{h}_i^{(j)}$ can be obtained from sequentially projecting $\mathbf{h}_i^{(j)}$ onto the sequential orthogonal spaces associated with the channel vectors of $\mathcal{G}_1, \mathcal{G}_2, \dots, \mathcal{G}_{j-1}, \mathcal{G}_{j+1}, \dots, \mathcal{G}_{N_g}$, as discussed in Lemma 1 and Example 1, i.e., $\mathbf{g}_i^{(j)} = \mathcal{P}(\mathcal{G}_{N_g} | \mathcal{G}_{N_g-1}, \dots, \mathcal{G}_{j+1}, \mathcal{G}_{j-1}, \dots, \mathcal{G}_1) \cdots \mathcal{P}(\mathcal{G}_{j+1} | \mathcal{G}_{j-1}, \dots, \mathcal{G}_1) \mathcal{P}(\mathcal{G}_{j-1} | \mathcal{G}_{j-2}, \dots, \mathcal{G}_1) \cdots \mathcal{P}(\mathcal{G}_2 | \mathcal{G}_1) \mathcal{P}(\mathcal{G}_1) \mathbf{h}_i^{(j)}$, where $\mathcal{P}(\mathcal{B} | \mathcal{A})$ denotes the sequential projection onto the orthogonal space of the projected subspace of \mathcal{B} onto $\mathcal{C}^\perp(\mathcal{A})$. (Please see Lemma 1 and Example 1.) Here, we have $N_g - 1$ projection stages. At each projection stage, the proposed user grouping algorithm, Algorithm 1, guarantees that norm reduction is not beyond $(1 - \theta^{th})$. The norm of the ZF effective channel can be written as (see Example 1)

$$\|\mathbf{g}_i^{(j)}\|^2 = Y \|\mathbf{h}_i^{(j)}\|^2, \quad (81)$$

where the reduction gain random variable Y depends on the channels, but $(1 - \theta^{th})^{K-1} =: Y^{th} \leq Y \leq 1$ since $N_g \leq K$. By (81) and Lemma 3 below, we have the claim (33). ■

Lemma 3: Let X be a random variable satisfying the condition, $\lim_{x \rightarrow 0} \frac{\log \Pr(X \leq x)}{\log x} = d$, and let Y be a random variable satisfying the condition, $Y^{th} \leq Y \leq 1$, where Y^{th} is some constant $\in (0, 1]$ and d is some positive constant. Then, the product $Z := XY$ satisfies $\lim_{z \rightarrow 0} \frac{\log \Pr(Z \leq z)}{\log z} = d$.

Proof of Lemma 3:

$$\begin{aligned} \Pr(X \leq z) &\leq \Pr(Z \leq z) \leq \Pr(Y^{th} X \leq z) \\ \Leftrightarrow \Pr(X \leq z) &\leq \Pr(Z \leq z) \leq \Pr(X \leq \frac{z}{Y^{th}}) \\ \Leftrightarrow \lim_{z \rightarrow 0} \frac{\log \Pr(X \leq z)}{\log z} &\leq \lim_{z \rightarrow 0} \frac{\log \Pr(Z \leq z)}{\log z} \leq \lim_{z \rightarrow 0} \frac{\log \Pr(X \leq \frac{z}{Y^{th}})}{\log z} \\ \Leftrightarrow \lim_{z \rightarrow 0} \frac{\log \Pr(X \leq z)}{\log z} &\leq \lim_{z \rightarrow 0} \frac{\log \Pr(Z \leq z)}{\log z} \leq \lim_{z \rightarrow 0} \frac{\log \Pr(X \leq \frac{z}{Y^{th}})}{\log \frac{z}{Y^{th}}} \cdot \frac{\log \frac{z}{Y^{th}}}{\log z} \\ \Leftrightarrow d &\leq \lim_{z \rightarrow 0} \frac{\log \Pr(Z \leq z)}{\log z} \leq d, \end{aligned} \quad (82)$$

where (82) holds because $Y^{th} X \leq Z = YX \leq X$ due to $Y \in (Y^{th}, 1)$. Therefore, the claim follows. ■

APPENDIX D: EXISTENCE OF POWER DISTRIBUTION FACTORS

Lemma 4: There always exists a collection of in-group power distribution factors $(\delta_1^{(j)}, \dots, \delta_\ell^{(j)})$ for \mathcal{G}_j with $|\mathcal{G}_j| = \ell$ such that $(\frac{\delta_i^{(j)}}{2^{R^{th}-1}} - \sum_{m=1}^{i-1} \delta_m^{(j)})$ in (56) is strictly positive for all $i = 2, \dots, \ell$.

Proof: The condition is equivalent to the following:

$$\frac{\delta_i^{(j)}}{2^{R^{th}} - 1} - \sum_{m=1}^{i-1} \delta_m^{(j)} > 0 \Leftrightarrow \frac{\delta_i^{(j)}}{\sum_{m=1}^{i-1} \delta_m^{(j)}} > 2^{R^{th}} - 1, \quad i = 2, \dots, \ell \quad (83)$$

Consider the following recursion

$$\delta_i^{(j)} = (2^{R^{th}} - 1 + C)(\delta_1^{(j)} + \dots + \delta_{i-1}^{(j)}), \quad (84)$$

where $C > 0$ is an arbitrary positive constant. It is easy to see that any solution to (84) satisfies (83).

Solving the recursion yields

$$\delta_i^{(j)} = \delta_1^{(j)}(2^{R^{th}} - 1 + C)(2^{R^{th}} + C)^{i-2}. \quad (85)$$

With normalization for $\sum_{i=1}^{\ell} \delta_i^{(j)} = 1$, we have

$$\delta_1^{(j)} = \frac{1}{(2^{R^{th}} + C)^{\ell-1}}, \quad \text{and} \quad \delta_i^{(j)} = \frac{2^{R^{th}} - 1 + C}{(2^{R^{th}} + C)^{\ell-i+1}}, \quad i = 2, \dots, \ell, \quad (86)$$

and all $\delta_i^{(j)} \geq 0$. Hence, we have a collection of power distribution factors for the condition. ■

APPENDIX E: SCALABLE ADAPTIVE USER GROUPING

We need the angle between the channel subspaces of any two user groups be larger than a certain threshold. This guarantees that inter-group ZF does not harm the diversity order. A scalable adaptive user grouping method for this purpose can be devised based on the semi-orthogonal user selection (SUS) algorithm in [4].

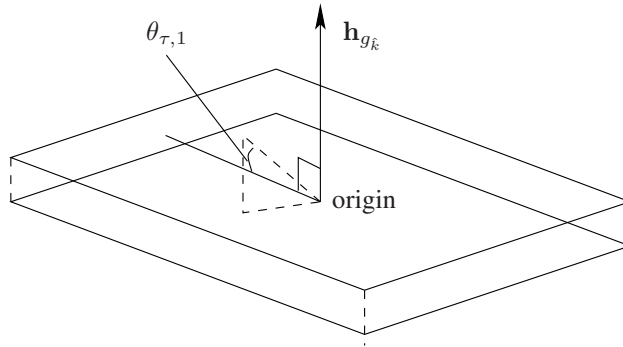


Fig. 11: A hyperslab constructed based on a channel vector (the dotted line segment from the origin to the plane has length one)

First, we predetermine two angle threshold values $\theta_{\tau,1} \in (0, \pi/2)$ and $\theta_{\tau,2} \in (0, \pi/2)$ such that

$\theta_{\tau,2} < \frac{\pi}{2} - \theta_{\tau,1}$. With the channel vectors $\mathbf{h}_k, k = 1, 2, \dots, K$ in \mathbb{C}^N , like in the SUS algorithm,[‡] we first select the user that has the largest channel magnitude. Without loss of generality, we assume the index of the first selected user is k_1 . Then, based on the CSI \mathbf{h}_{k_1} , we construct a user-selection hyperslab defined as

$$\mathcal{H}_1 = \left\{ \mathbf{h} \in \mathbb{C}^N : \frac{|\mathbf{h}_{k_1}^H \mathbf{h}|}{\|\mathbf{h}_{k_1}\| \cdot \|\mathbf{h}\|} \leq \gamma \right\}, \quad (87)$$

as shown in Fig. 11, where the value γ is determined to satisfy the following relationship with the angle $\theta_{\tau,1}$ in Fig. 11:

$$\gamma = \cos \left(\frac{\pi}{2} - \theta_{\tau,1} \right).$$

Note that if a vector \mathbf{h} is contained in \mathcal{H}_1 , \mathbf{h} is semi-orthogonal to \mathbf{h}_{k_1} with the angle between \mathbf{h}_{k_1} and \mathbf{h} being in $[\frac{\pi}{2} - \theta_{\tau,1}, \frac{\pi}{2} + \theta_{\tau,1}]$. Then, we select the user whose channel vector is contained in the hyperslab \mathcal{H}_1 and who has maximum channel vector magnitude within \mathcal{H}_1 . After the second user is selected, another hyperslab is constructed based on its channel vector. The third user is selected as the user with maximum channel norm within the intersection of the first and second hyperslabs and this guarantees that the third user's channel vector is semi-orthogonal to both first and second users' channel vectors with minimum angle separation of $\frac{\pi}{2} - \theta_{\tau,1}$. We continue this procedure until either we cannot find any user in the intersection or we reach the final K -th user. This is basically the SUS algorithm. If the procedure reaches the K -th user, we have K user groups each with one user and the constructed K groups satisfy the required angle separation property. If the procedure stops at the N'_g -th step before reaching the K -th user, then we construct N'_g candidate user groups. At this point, each candidate user group has one user obtained from the SUS algorithm.

Now consider the remaining $K - N'_g$ users. Each of the remaining $K - N'_g$ users' channels should be close to one of the channels of the N'_g users obtained by the SUS procedure with angle less than $\frac{\pi}{2} - \theta_{\tau,1}$. Otherwise, one separate group had been constructed in the above SUS stage. Let the remaining $K - N'_g$ users be named Users $u_1, u_2, \dots, u_{K-N'_g}$. Now, pick User u_1 and compute the angle between the channel of User u_1 and the channel of each of the N'_g users obtained by the above SUS stage. Let the angles be $\{\theta_1^{(1)}, \theta_2^{(1)}, \dots, \theta_{N'_g}^{(1)}\}$. Assign User u_1 to the group with the smallest angle distance. Furthermore, combine the groups

$$\{\mathcal{G}_j \mid j = 1, \dots, N'_g \text{ and } \theta_j^{(1)} < \theta_{\tau,2}\} \quad (88)$$

[‡]The explanation of the SUS algorithm here is adapted from [4], [7].

as a single group. That is, if the minimum angle is not guaranteed between groups due to the inclusion of User u_1 , then combine the groups violating the minimum angle distance condition. Suppose that the assigned group is Group 1 without loss of generality and still all groups satisfy the minimum angle distance condition. Now, pick User u_2 and compute the angle between the channel of User u_2 and the channel of each of the N'_g groups. Since we have two users in Group 1, we compute two angle values between User u_2 and the two users of Group 1 and denote them by $\theta_{11}^{(2)}$ and $\theta_{12}^{(2)}$. Let the angle between User u_2 and the single user in each user of Groups $2, \dots, N'_g$ be $\theta_2^{(2)}, \dots, \theta_{N'_g}^{(2)}$. Compute the minimum of $\{\theta_{11}^{(2)}, \theta_{12}^{(2)}, \theta_2^{(2)}, \dots, \theta_{N'_g}^{(2)}\}$ and assign User u_2 to the group that has the user with the minimum angle distance from User u_2 . Again, combine the groups violating the minimum angle condition due to the inclusion of User u_2 by similar computation to (88) with the same threshold $\theta_{\tau,2}$. After that, continue to User u_3 . We continue this procedure until User $u_{K-N'_g}$ is assigned. Finally, the procedure will return $N_g(\leq N'_g)$ groups.

The above method guarantees the minimum angle $\theta_{\tau,2}$ between any two groups and is scalable with respect to K since the SUS algorithm is sequential and angle checking of the remaining $K - N'_g$ users with the N'_g groups requires at most K^2 checkings.

We actually implemented this grouping idea and the result is shown in Fig. 12. We did not fine-tune the two parameters. It seems that more tweaking is necessary for stable performance. However, it is observed that the new approach also yields far better outage performance as expected. Indeed, more efficient user grouping algorithms for the desired purpose can be devised.

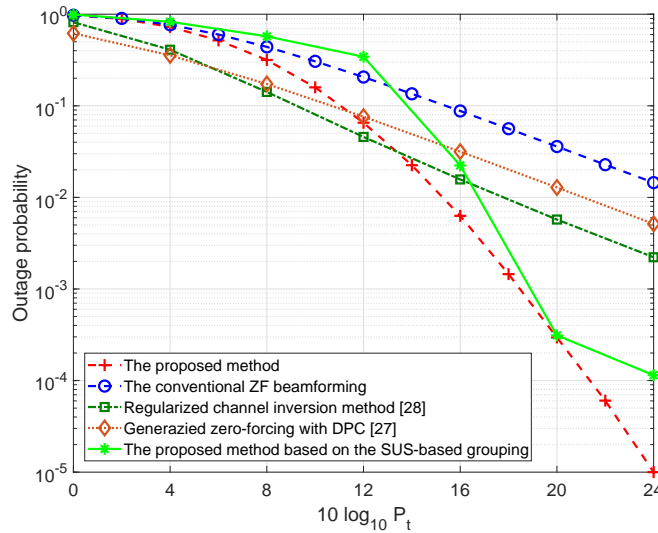


Fig. 12: Outage probability of several methods: The SUS-based grouping with $\theta_{\tau,1} = 0.25$ and $\theta_{\tau,2} = 0.55$

REFERENCES

- [1] J. Seo, “Beamformer design based on non-linear reception in MIMO downlink system,” *PhD Dissertation*, KAIST, Aug. 2018.
- [2] H. Weingarten, Y. Steinberg, and S. Shamai, “The capacity region of the Gaussian multiple-input multiple-output broadcast channels,” *IEEE Trans. Inf. Theory*, vol. 52, pp. 3936–3964, Sep. 2009.
- [3] M. Sharif and B. Hassibi, “On the capacity of MIMO broadcast channels with partial side information,” *IEEE Trans. Inf. Theory*, vol. 51, pp. 506–522, Feb. 2005.
- [4] T. Yoo and A. Goldsmith, “On the optimality of multiantenna broadcast scheduling using zero-forcing beamforming,” *IEEE J. Sel. Areas in Commun.*, vol. 24, pp. 528–541, Mar. 2006.
- [5] 3GPP, “Evolved universal terrestrial radio access (E-UTRA): Downlink multiple input multiple output (MIMO) enhancement for LTE-Advanced (Release 11),” *TR 36.871, V11.0.0*, 2011-2012.
- [6] Q. H. Spencer, A. L. Swindlehurst, and M. Haardt, “Zero-forcing methods for downlink spatial multiplexing in multiuser MIMO channels,” *IEEE Trans. Signal Process.*, vol. 52, pp. 461 – 471, Feb. 2004.
- [7] G. Lee and Y. Sung, “A new approach to user scheduling in massive multi-user MIMO broadcast channels,” *IEEE Trans. Commun.*, vol. 66, pp. 1481 – 1495, Apr. 2018.
- [8] G. Lee, Y. Sung, and J. Seo, “Randomly-directional beamforming in mm-wave multi-user MISO downlink,” *IEEE Trans. Wireless Commun.*, vol. 15, pp. 1086–1100, Feb. 2016.
- [9] G. Lee, Y. Sung, and M. Kountouris, “On the performance of random beamforming in sparse millimeter wave channels,” *IEEE J. Sel. Topics Signal Process.*, vol. 10, pp. 560–575, Apr. 2016.
- [10] H. Huh, A. M. Tulino, and G. Caire, “Network mimo with linear zero-forcing beamforming: Large system analysis, impact of channel estimation, and reduced-complexity scheduling,” *IEEE Trans. Inf. Theory*, vol. 58, pp. 2911–2934, Dec. 2012.
- [11] Y. Saito, Y. Kishiyama, A. Benjebbour, T. Nakamura, A. Li, and K. Higuchi, “Non-orthogonal multiple access (NOMA) for cellular future radio access,” in *Proc. IEEE VTC*, pp. 1–5, Jun. 2013.
- [12] Y. Mao, B. Clerckx, and V. O. Li, “Rate-splitting multiple access for downlink communication systems: bridging, generalizing, and outperforming sdma and noma,” *EURASIP Journal on Wireless Communications and Networking*, vol. 2018, no. 1, p. 133, 2018.
- [13] J. Seo and Y. Sung, “A new transceiver architecture for multi-user MIMO communication based on mixture of linear and non-linear reception,” in *Proc. SPAWC*, (Sapporo, Japan), Jun. 2017.
- [14] Z. Chen, Z. Ding, and X. Dai, “Beamforming for combating inter-cluster and intra-cluster interference in hybrid NOMA systems,” *IEEE Access*, vol. 4, pp. 4452 – 4463, Aug. 2016.
- [15] J. Kazemitabar and H. Jafarkhani, “Multiuser interference cancellation and detection for users with more than two transmit antennas,” *IEEE Trans. Commun.*, vol. 56, no. 4, pp. 574 – 583, 2008.
- [16] A. Adhikary, J. Nam, J. Ahn, and G. Caire, “Joint spatial division and multiplexing – The large-scale array regime,” *IEEE Trans. Inf. Theory*, vol. 59, pp. 6441 – 6463, Oct. 2013.
- [17] D. Tse and P. Viswanath, *Fundamentals of Wireless Communication*. Cambridge University Press, 2005.
- [18] M. F. Hanif, Z. Ding, T. Ratnarajah, and G. K. Karagiannidis, “A minorization-maximization method for optimizing sum rate in the downlink of non-orthogonal multiple access systems,” *IEEE Trans. Signal Process.*, vol. 64, no. 1, pp. 76–88, 2016.
- [19] A. L. Yuille and A. Rangarajan, “The concave-convex procedure,” *Neural computation*, vol. 15, no. 4, pp. 915–936, 2003.

- [20] J. Seo and Y. Sung, “Beam design and user scheduling for non-orthogonal multiple access with multiple antennas based on Pareto-optimality,” *IEEE Trans. Signal Process.*, vol. 66, pp. 2876 – 2891, Jun. 2018.
- [21] R. Zhang and S. Cui, “Cooperative interference management with miso beamforming,” *IEEE Trans. Signal Process.*, vol. 58, pp. 5450 – 5458, Oct. 2010.
- [22] S. Ali, E. Hossain, and D. I. Kim, “Non-orthogonal multiple access (NOMA) for downlink multiuser MIMO systems: User clustering, beamforming, and power allocation,” *IEEE Access*, vol. 5, pp. 565 – 577, 2017.
- [23] J. Hou, J. E. Smee, H. D. Pfister, and S. Tomasin, “Implementing interference cancellation to increase the EV-DO Rev A reverse link capacity,” *IEEE Communications Magazine*, vol. 44, pp. 58 – 64, Feb. 2006.
- [24] Z. Ding, F. Adachi, and H. V. Poor, “The application of MIMO to non-orthogonal multiple access,” *IEEE Trans. Wireless Commun.*, vol. 15, pp. 537 – 552, Jan. 2016.
- [25] L. Zheng and D. N. C. Tse, “Diversity and multiplexing: a fundamental tradeoff in multiple-antenna channels,” *IEEE Trans. Inf. Theory*, vol. 49, pp. 1073 – 1096, May 2003.
- [26] L. Mroueh, S. R.-Leveil, G. R.-Ben Othman, and J.-C. Belfiore, “Dmt of weighted parallel channels: Application to broadcast channels,” in *Proc. ISIT*, Jul. 2008.
- [27] S. Hu and F. Rusek, “A generalized zero-forcing precoder with successive dirty-paper coding in MISO broadcast channels,” *IEEE Trans. Wireless Commun.*, vol. 16, pp. 3632 – 3645, Jun. 2017.
- [28] C. B. Peel, B. M. Hochwald, and A. L. Swindlehurst, “A vector-perturbation technique for near-capacity multiantenna multiuser communication-part I: Channel inversion and regularization,” *IEEE Trans. Commun.*, vol. 53, pp. 195 – 202, Jan. 2005.
- [29] N. Jindal, “MIMO broadcast channels with finite-rate feedback,” *IEEE Trans. Inf. Theory*, vol. 52, pp. 5045 – 5060, Nov. 2006.
- [30] Y. Zeng, C. M. Yetis, E. Gunawan, Y. L. Guan, and R. Zhang, “Transmit optimization with improper Gaussian signaling for interference channels,” *IEEE Trans. Signal Process.*, vol. 61, pp. 2899 – 2913, Jun. 2013.
- [31] N. D. Sidiropoulos, T. N. Davidson, and Z.-Q. Luo, “Transmit beamforming for physical-layer multicasting,” *IEEE Trans. Signal Process.*, vol. 54, no. 6, pp. 2239–2251, 2006.
- [32] Z.-Q. Luo, N. D. Sidiropoulos, P. Tseng, and S. Zhang, “Approximation bounds for quadratic optimization with homogeneous quadratic constraints,” *SIAM Journal on optimization*, vol. 18, no. 1, pp. 1–28, 2007.